INFORMATION TO USERS

This dissertation was produced from a microfilm copy of the original document. While the most advanced technological means to photograph and reproduce this document have been used, the quality is heavily dependent upon the quality of the original submitted.

The following explanation of techniques is provided to help you understand markings or patterns which may appear on this reproduction.

1. The sign or "target" for pages apparently lacking from the document photographed is "Missing Page(s)". If it was possible to obtain the missing page(s) or section, they are spliced into the film along with adjacent pages. This may have necessitated cutting thru an image and duplicating adjacent pages to insure you complete continuity.

2. When an image on the film is obliterated with a large round black mark, it is an indication that the photographer suspected that the copy may have moved during exposure and thus cause a blurred image. You will find a good image of the page in the adjacent frame.

3. When a map, drawing or chart, etc., was part of the material being photographed the photographer followed a definite method in "sectioning" the material. It is customary to begin photoing at the upper left hand corner of a large sheet and to continue photoing from left to right in equal sections with a small overlap. If necessary, sectioning is continued again — beginning below the first row and continuing on until complete.

4. The majority of users indicate that the textual content is of greatest value, however, a somewhat higher quality reproduction could be made from "photographs" if essential to the understanding of the dissertation. Silver prints of "photographs" may be ordered at additional charge by writing the Order Department, giving the catalog number, title, author and specific pages you wish reproduced.

University Microfilms

300 North Zeeb Road
Ann Arbor, Michigan 48106

A Xerox Education Company

72-24,130

GOLDGRABEN, J. Richard, 1934-

HYDRODYNAMIC MODELS OF WATER AND SOLUTE TRANSPORT IN CHANNELS AND EXIT MIXING REGIONS OF EPITHELIAL CELL LAYERS.

The City University of New York, Ph.D., 1972
Engineering, mechanical

HYDRODYNAMIC MODELS OF WATER AND SOLUTE TRANSPORT IN CHANNELS AND EXIT MIXING REGIONS OF EPITHELIAL CELL LAYERS

by

J.RICHARD GOLDGRABEN

A dissertation submitted to the Graduate Faculty in Engineering in partial fulfillment of the requirements for the degree of Doctor of Philosophy, The City University of New York

1972

This manuscript has been read and accepted for the Graduate Faculty in Engineering in satisfaction of the dissertation requirement for the degree of Doctor of Philosophy.

5/11/72
date

Sheldon Weinbaum
Chairman of Examining Committee

5/11/72
date

Jacques E. Bouvenste
Executive Officer

Professor R. Graff, co-mentor
Professor I. Leopold
Professor C.M. Tchen
Professor S. Weinbaum, mentor
Supervisory Committee

The City University of New York

DEDICATION

To my wife Ann and to Bonnie and Marcie who have stood beside me with encouragement and understanding during these years when too little of my time was spent in being a husband and a father and to my Parents who labor in my struggles and rejoice in my successes, I dedicate this work with love and affection.

ACKNOWLEDGEMENT

I wish to express my sincere appreciation to my mentor Dr. Sheldon Weinbaum for his guidance and for sharing with me his profound understanding of the mathematical and physical sciences throughout the course of study which has culminated in this research effort. I also want to thank Dr. Robert Graff of the City College of New York, my co-mentor, and Drs. Maurice Langham and Keith Green of the Wilmer Institute, Johns Hopkins University School of Medicine for their many helpful discussions and insights. This work was supported in part by a National Science Foundation Science Faculty Fellowship.

CONTENTS

LIST OF ILLUSTRATIONS

CHAPTER 1 INTRODUCTION

1.1 Physiological Background

Epithelial cell layers line the surfaces of many human, animal and insect organs such as the ciliary body of the eye, gall bladder, frog skin, avian salt gland and renal collecting tubules, to mention a few, and have the primary function of transporting water and solutes between the serosal fluids in the capillary beds and the mucosal fluids in the lumen or cavities of these organs. Physiologists have for many years sought to explain the intriguing ability of these epithelia to produce flow of water and solute against or in the absence of electrochemical driving forces between the mucosal and serosal bathing fluids. It now appears, as a result of electron-micrographic studies, experimental measurements of in vivo and in vitro membrane transport rates and newly developed mathematical hydrodynamic diffusion models that the unique features of epithelial transport are due to the specialized nature of the epithelial ultrastructure and to the presence of localized driving forces. While different epithelial cell layers exhibit considerable diversity in their function and ultrastructure, all appeal to possess long tortuous extracellular channels between adjacent cells and metabolically linked ion pumps which are the source of the so-called active transport. The width of the channels ranges from 50 to 200Å, depending on the membrane system and the degree of dilation due to transport of fluid through them. This is roughly two orders of magnitude larger than the diameters of the solvent and solute molecules. Cell sizes and, hence, the length of the channels also vary, with 20 μ being a representative linear dimension.

Figure 1 is a schematic taken from Diamond and Tormey (1966) and shows what one would observe in an electron-micrograph of the gall bladder epithelium. This membrane is a simple monolayer. The movement of water and salt across the membrane from the lumen or sac interior is

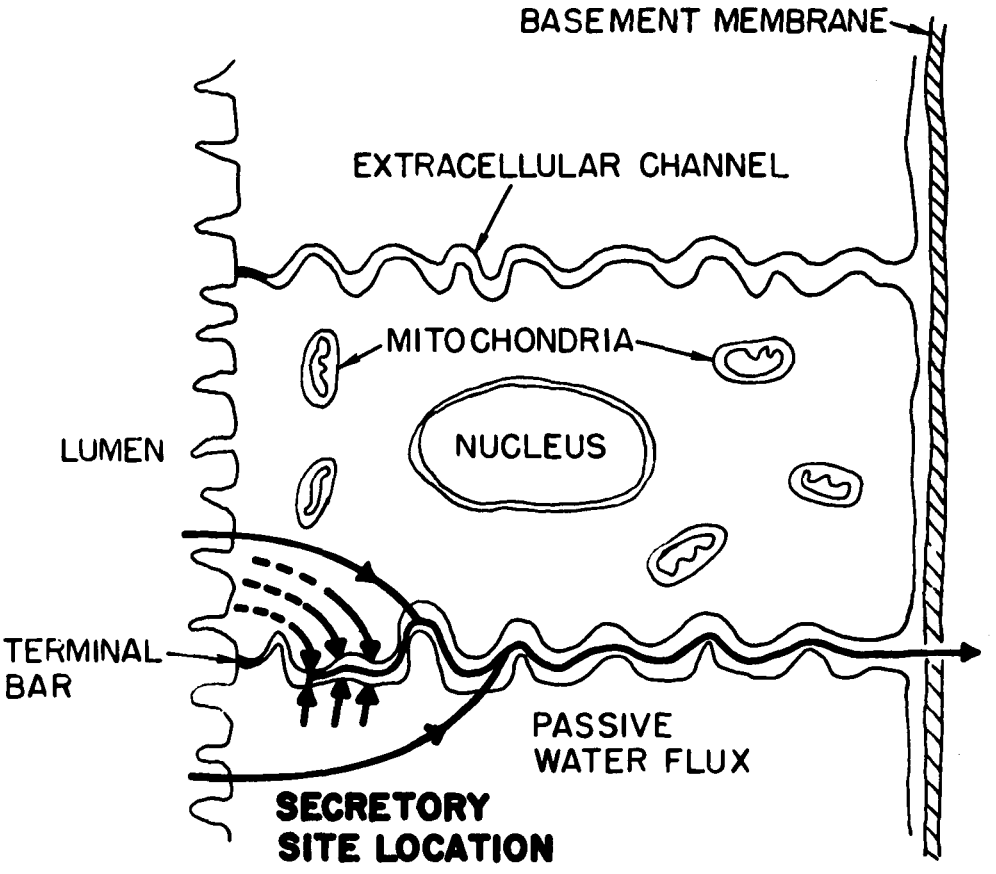

Figure 1. Schematic Diagram of Gall Bladder Epithelial Membrane (Based on Diamond and Tormey, 1966)

hypothesized to occur via the extracellular channels which are closed at their lumenal ends by junctional complexes or terminal bars. These complexes are assumed to form a solute and water tight seal and the membrane is therefore considered to be non-porous. The energy for the water and solute movement derives from sodium ion pumps which histochemical studies show are located near the closed ends of the channel within the relatively semipermeable intercellular membranes that form the channel boundaries. The local osmotic gradient established across the intercellular membrane by the pumping action draws water passively from the cell interior into the channel. To conserve mass, both solute and water are foced out the open end of the channel due to the build up of pressure at the closed end. For steady state operation both the water and salt are replenished from the inner bathing solution in the lumen. The intriguing feature of gall bladder transport is that the fluid exuding from the channel exit is, over a wide concentration range, isotonic with the salt solution in the lumen, and that transport occurs in the absence of a transmembrane pressure differential, Diamond (1964). Other membranes, such as the avian salt gland, teleost intestine, and the ciliary processes, transport a slightly hypertonic fluid.

The active transport of sodium ions in the gall bladder is accompanied by an equal movement of chloride ions which maintains electroneutraility between the serosal and mucosal surfaces. In other epithelia the movement of the anion or cation may be partially or totally inhibited. The ion pump then acts as a battery which produces charge separation and a potential difference across the membrane. Such electrical effects cannot be examined by the two specie (solute, solvent) model developed in the present work. A three specie model describing separate anion, cation and solvent transport is required.

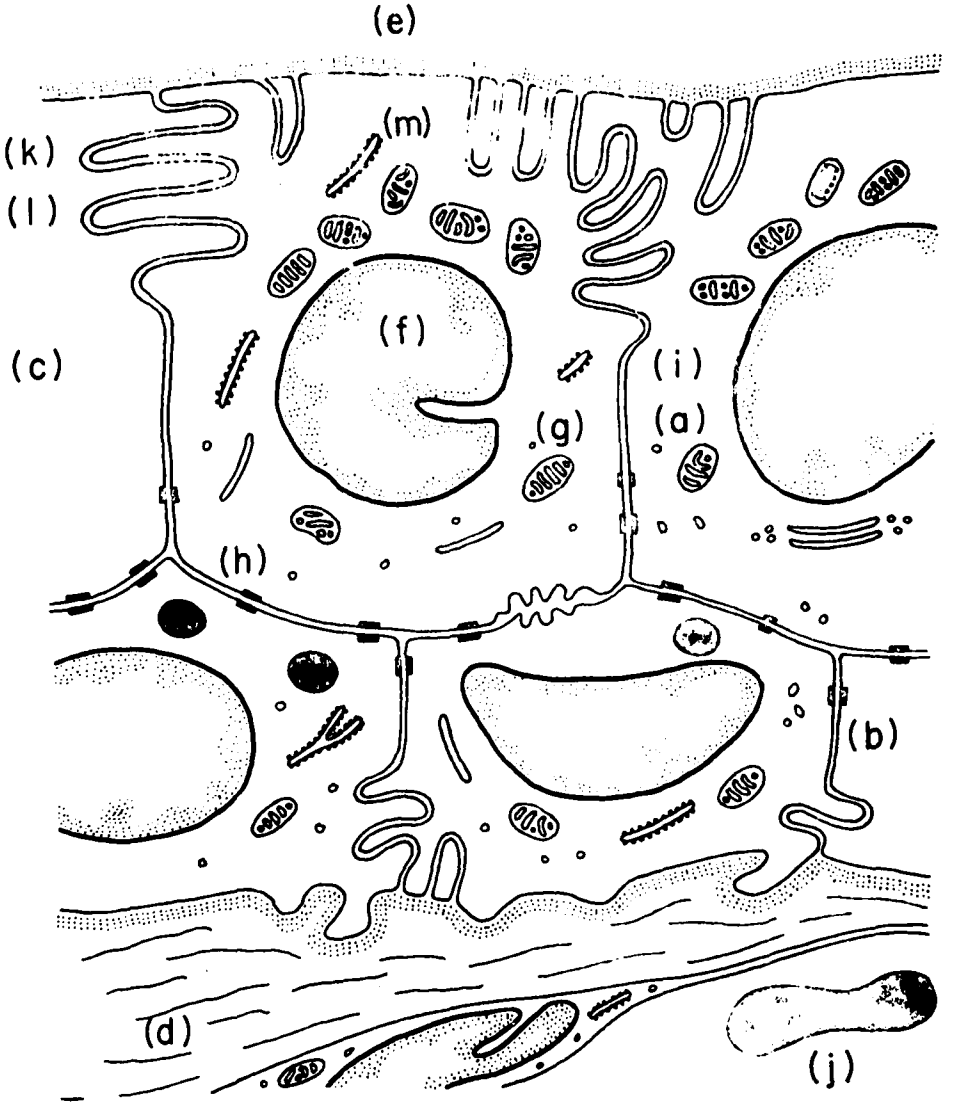

Figure 2. Schematic Diagram of Ciliary Body Epithelial Membrane showing: (a) extracellular channels, (b) pigmented layer, (c) non-pigmented layer, (d) stromal fluid, (e) posterior chamber fluid, (f) cell nuclei, (g) mitochondria, (h) desmosomes, (i) partially occluded zones, (j) red blood cell, (k) proposed secretory site based on ATPase activity, (l) lateral inflodings, (m) apical infoldings.

In contrast to the relatively simple gall bladder monolayer depicted in Figure 1, Figure 2 shows schematically the ultrastructure observed in an electron micrograph of the considerably more complex epithelium in the ciliary precesses of the eye. This membrane secretes a salt solution called aqueous humor into the posterior chamber behind the lens at a relatively high rate which ranges from 0.4 to 3μl min^{-1} cm^{-2} for human and cat eyes respectively. The membrane is a dual cell layer comprised of pigmented and nonpigmented cells. While the details of the membrane ultrastructure are not as well documented as that of the gall bladder, there is a significant body of evidence to suggest that the extracellular channels provide a direct link between the serosal (stromal) and mucosal (posterior chamber) fluids, but contain partially occluded zones whose physiological function is not understood. The apical infoldings shown in the diagram are actually interface projections of adjacent cells above and below the plane of the micrograph. Histochemical studies of AT Pase activity show that the sites of active ion transport are located largely in the lateral infoldings of the nonpigmented cell layer. Thus, the position of the secretory sites relative to the channel exit are opposite that of the gall bladder.

In the absence of junctional complexis both water and solute will have finite fluxes at the channel entrance. Excluding electrical effects, two additional driving forces for the channel flow, which were not present in the gall bladder, must be considered. Thus, three driving forces of non-electrical origin can be anticipated to contribute to the total water and solute movement in porous epithelia with secretory sites; active transport due to the ion pump (local osmosis), concentration difference between serosal and mucosal bathing solutions (osmosis), and filtration due to the hydrodynamic pressure difference between the interstitial pressure in the stromal fluid and the intraocular pressure in the posterior chamber.

One important and heretofore unexplained feature of ciliary body transport which the present study will attempt to answer, is the large and disproportionate difference in the measured water and solute fluxes in living and excised eyes of both the cat and rabbit. In the experiments of Cole (1961) (1962), for example, the measured aqueous flux in vivo was five times greater than that in excised preparations while the sodium flux in vivo was only 50 percent greater than that in the preparation. In addition, active transport accounted for all of the sodium flux in the excised preparation while accounting for only 30% in vivo.

One cannot obtain a complete picture of epithelial transport without considering the mixing process which ensues when the effluent from the extracellular channels enters the outer bathing solution. A schematic diagram of a typical exit region is shown in Figure 3. The channel effluent encounters an outer bathing solution which may be relatively quiescent as in the ciliary processes, well stirred as is the case of many experiments performed with excised preparations, or which may possess a variety of convective velocity distributions depending on the particular membrane system. A typical epithelial cell layer contains an array of channels each producing a so-called low Reynolds number jet which interacts with adjacent jets, with the outer bathing solution and with any solute or solvent flux (Q_e in Figure 3) which may be created across a permeable outer cell membrane by osmotic differentials.

The objective of the present work is the development of mathematical models to describe the transport phenomena in the extracellular channels of porous and non-porous epithelia and the mixing process that occurs in the channel exit region. The interested reader is referred to Stein (1967) and Bittar (1970) for more complete discussions of membrane transport.

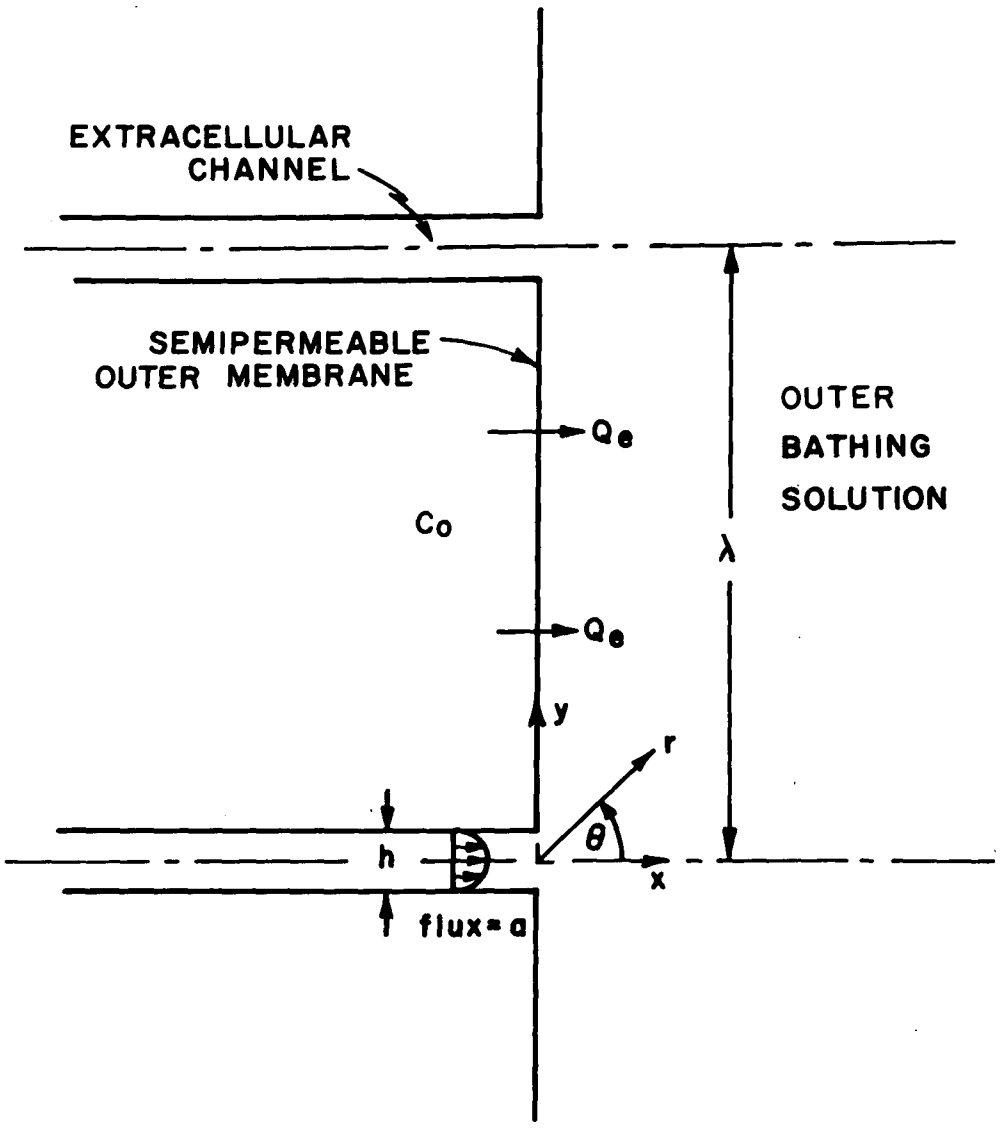

Figure 3. Schematic Diagram of Epithelial Exit Mixing Region

1.2 Previous Models

Diamond and Bossert (1967), hereafter referred to as D&B, have formulated an ingeneous mathematical model to describe the so-called standing gradient osmotic flow which is established in the channels of non-porous epithelia where there is no filtration. Porous membrane systems such as that depicted in Figure 2 have not previously been studied using theoretical models. The model developed by D&B to describe the behavior of the gall bladder treats the extracellular channel as a one-dimensional flow in a constant area cylindrical pore of circular cross section. Both the solute and total mass are conserved in the channel interior, while the lateral boundary conditions allow for active transport of salt and passive movement of water, but not salt, across the intercellular membranes. Both the water and solute fluxes at the closed end (initial station) are zero while the concentration C_{so} in the cell interior is assumed well mixed and hence uniform. The boundary value problem just described is not unique since the initial concentration $C_s(0)$ can take on any value. In D&B, $C_s(0)$ is uniquely determined for a channel of given length L by requiring that the dimensionless exit concentration $C_s(L) = 1$, that is, that the channel effluent be isotonic with the solution in the cell interior. This is one of the weaknesses of the D&B model since in reality $C_s(L)$ can have any value. It is neither the concentration of a well stirred outer bathing solution (a concentration boundary layer could exist) or the concentration that would be measured if the effluent were allowed to drip off the gall bladder sac and be collected in a beaker. The latter concentration is given by $\frac{Q_s(L)}{Q(L)}$, where $Q_s(L)$ and $Q(L)$ are the total solute and water fluxes at the channel exit; $Q_s(L)$ includes both a convective and a diffusional component unless $\frac{dC_s(L)}{dx} = 0$. Therefore, in specifying $C_s(L)$, one has unecessarily

constrained the channel flow behavior. For this reason no exit boundary condition is prescribed in the analysis presented in Chapter 2 but rather, $C_s(0)$ varied as free parameter, each assumed initial concentration yielding a different solution. One will observe later that this extra degree of freedom will lead to a new family of solutions that is not contained in the D&B analysis.

A fundamental question that is not answered by the standing gradient osmotic model for the gall bladder is how the water in the cell interior is replenished. It would seem reasonable to expect this water to be derived from the lumenal fluid, the transport occuring through a local osmotic gradient at the inner membrane. This requirement is not satisfied by the D&B model since the osmolarity of the lumenal fluid and that in the cell interior are assumed equal. For self consitency the condition of isotonic transport in Diamond's (1964) experiments would appear to require that the concentration of the lumenal fluid be hypotonic relative to the solution in the cell interior and isotonic with respect to both the channel effluent and the outer bathing solution. The latter requires that a concentration boundary layer not exist at the channel exit, hence that $dC_s(L)/dx = 0$. Thus, in contrast to D&B, one asks whether it is possible for a finite length channel to have an effluent which is hypotonic relative to the cell interior solution and at the same time have a vanishing gradient at the exit plane. The results presented in Chapter 2 show that such a condition is impossible for the model as presently formulated.

Approximate analytic solutions to D&B's equations and boundary conditions based on a small parameter expansion have been presented by Segel (1970). The governing equations are non-dimensionalized in a manner similar to that presented herein and the basic dimensionless groupings that characterize the D&B model are derived. These solutions compare well with D&B's numerical results over most of the anticipated range of values

for the membrane parameters.

Laminar and turbulent jet mixing problems at highRe have long been of interest to fluid mechanicians because of their numerous applications in both compressible and incompressible flows. The jets issuing from the channel exits of most epithelia are, on the other hand, Stokes jets. The work done to date on low Re jets have had little relevance for biological flows since they have treated a pure fluid and have not considered biologically meaningful boundary conditions. The qualitative behavior of biological jet is much more subtle than for single component Stokes jets since it involves the interaction between several different transport processes that can occur on the same or different length scales depending on the relative values of the five different dimensionless groups $\frac{a}{\nu}$, $\frac{a}{D}$, $\frac{M_s C_o}{\rho}$, $\frac{\rho a}{P_w C_o h}$ and $\frac{\lambda}{h}$ that characterize the particular flow problem. Here a is the volume efflux per unit channel depth, ν the kinematic viscosity, D the mass diffusivity coefficient for solute in water, ρ the total mass density, M_s the solute molecular weight, C_o the solute molar concentration interior to the boundary, P_w the water permeability coefficient of the boundary, h the channel height and λ the channel spacing if an array of channels is considered. $\frac{a}{\nu}$ is therefore an exit Reynolds number, $\frac{a}{D}$ a ratio of convective to diffusional solute flux, $\frac{M_s C_o}{\rho}$ a solute solvent density ratio, $\frac{\rho a}{P_w C_o h}$ a ratio of the channel efflux to the local passive water flux at the boundary and $\frac{\lambda}{h}$ a dimensionless channel spacing. Typical values of these dimensionless numbers for epithelial membrane problems considered herein are:

$$\frac{a}{\nu} \approx O(10^{-6}),\ \frac{a}{D} \approx O(10^{-3}),\ \frac{M_s C_o}{\rho} \approx O(10^{-2}),\ \frac{\rho a}{P_w C_o h} \approx O(10^{2}),\ \frac{\lambda}{h} \approx O(10^{3}).$$

In general, two characteristic lengths other than λ and h are possible for low Re jets with $\frac{a}{\nu} << 1; \frac{D}{U_o}$, when U_o is the channel centerline velocity at the exit, and $\frac{\rho a}{P_w C_o}$. The length scale $\frac{D}{U}$ is a measure of the distance from the source at which the convective and diffusional terms

in the solute conservation equation become of comparable magnitude. This does not appear if $\frac{a}{D} \leq O(1)$ since there is then no inner length scale in which the solute transport is convection dominated. The length scale $\frac{\rho a}{P_w C_o}$ is a measure of the distance from the channel exit at which the passive water flux at the boundary becomes comparable to the local convective flux due to the exit source. From the typical values given in the last paragraph one concludes that there are three important characteristic lengths for the two-dimensional jets emanating from the extracellular channels of epithelial membranes, and that these lengths are ordered as $h << \frac{\rho a}{P_w C_o} << \lambda$.

On the inner scale h the passive movement of water across the outer membrane (Q_e in Figure 3) is a higher order effect and the primary transport process is the diffusional relaxation of the inhomogeneity in the exit concentration profile. On the intermediate scale $\frac{\rho a}{P_w C_o}$ the passive water flux Q_e at the outer boundary is important and causes lowest order changes in the streamline pattern and higher order convective corrections in the concentration distribution. On the largest length scale λ the flow problem is essentially that of a slow viscous flow with a periodic water flux boundary condition in the plane of the channel exits assuming the latter are equally spaced. Chapter 3 examines one relatively simple jet problem; the mixing of an inhomogeneous effluent from a single two dimensional channel with a quiescent bathing solution which occupies a half plane, bounded by a semipermeable membrane in the plane of the exit that allows for the passive transport of water but not of solute. The model for the channel flow provides the initial conditions on the solute concentration and water flux at the channel exit. The model developed in Chapter 3 is appropriate for the exit mixing regions of the gall bladder and ciliary body epithelia.

Section 3.5 discusses, as suggestions for future work models that would be appropriate for epithelia of other organs.

CHAPTER 2. CHANNEL FLOW

1. Introduction

This chapter presents the formulation of the mathematical boundary value problem that describes the transport phenomena occuring in the mathematical model of the generalized electroneutral extracellular channel shown schematically in Figure 4. One wishes to determine the various velocity, solute concentration and pressure fields that can emerge when varied boundary conditions are applied at the channel ends and along the intercellular membranes which form the lateral walls of the channel. The fluid in the channel is assumed to be a two specie continum of solute and solvent and to have two-dimensional field properties. The desired field descriptions could be obtained from the well-known partial differential equations for overall continuity, conservation of solute and the Navier-Stokes momentum equation. The use of such a system of exact equations involves, however, a degree of mathematical complexity which, in light of the present status of our understanding of the relevant physiological phenomena on a molecular level, does not seem justified. Accordingly, we shall develop instead a simplified description using integral techniques that will enable us to reduce the conservation relations for the channel to a system of ordinary differential equations satisfying appropriate boundary conditions. This approach permits us to retain an approximate two-dimensional description of the velocity and solute concentration fields, and therefore, allows us to study the shear stress distribution and the mixing normal to the lateral boundaries of the channel.

For the aforementioned purposes the channel is divided into a series of infinitesimal control volume elements of length Δx, unit depth and height h which is assumed to be a slowly varying function of the streamwise coordinate x. An active solute flux and a passive water flux are assumed to enter the volume element symmetrically across the lateral boundaries.

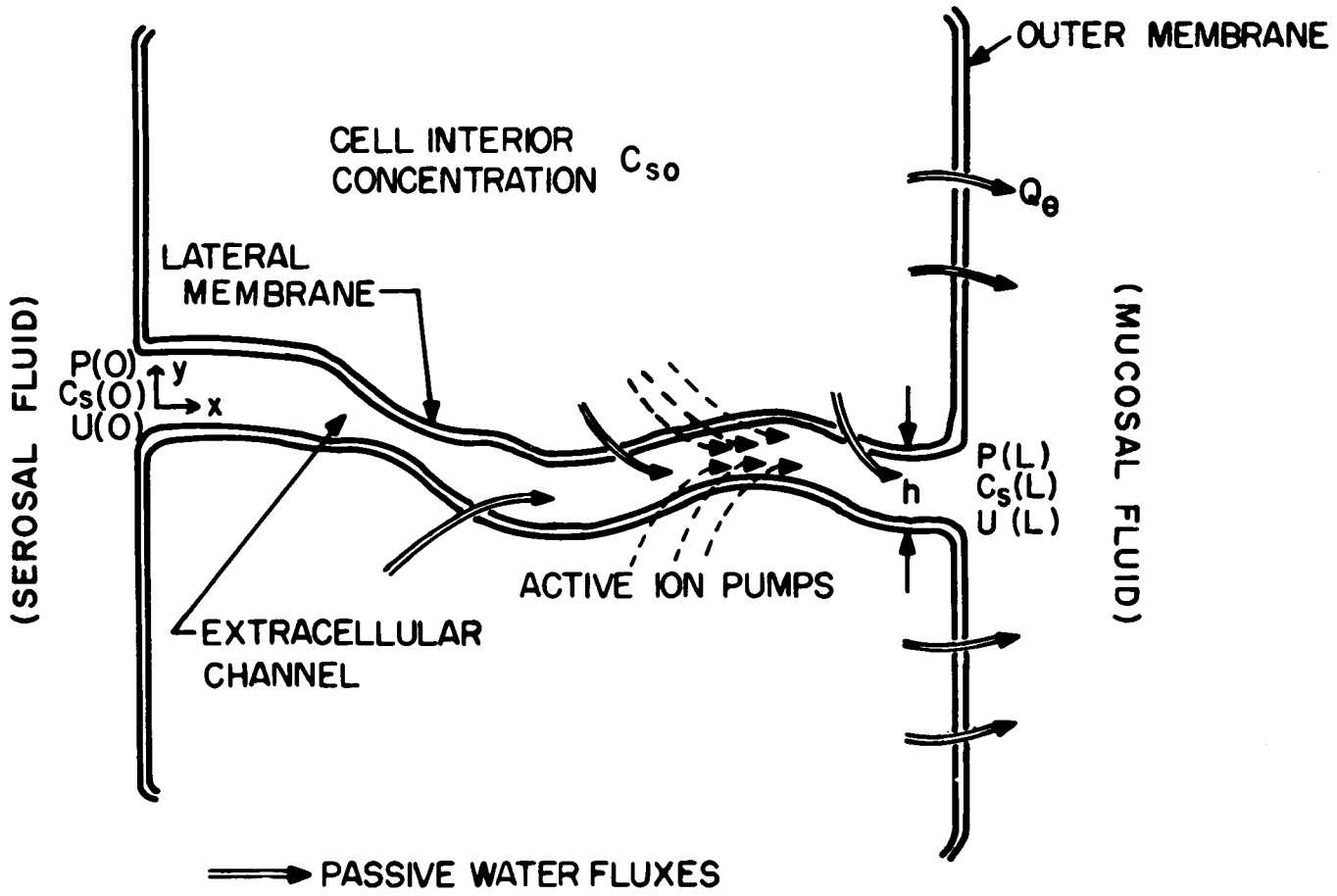

Figure 4. Generalized Extracellular Channel Model.

2 (a) Overall Continuity Equation

Conservation of total mass within the differential control volume of length Δx requires that the net mass flux of solute s and solvent w into the differential control volume be zero. Therefore,

$$\int_{-h(x)/2}^{+h(x)/2} (\rho_s u_s + \rho_w u_w)dy \Bigg|_{x=x} - \int_{-h(x+\Delta x)/2}^{+h(x+\Delta x)/2} (\rho_s u_s + \rho_w u_w)dy \Bigg|_{x=x+\Delta x} + (N(x) + F_s + F_w)\Delta x = 0 \qquad (2.1)$$

The notation in (2.1) has its usual meaning. $N(x)$ is the total active solute mass flux per unit length and depth entering a symmetrical channel from the active transport sites and F_w is the total passive flux of water crossing the two lateral membranes due to the local osmotic gradient. The intercellular membranes are assumed as in DξB to be sempermeable, although it is believed that this condition needs to be examined more critically, at least for the gall bladder. Thus, the passive solute flux F_s will be neglected.

The local mass average velocity u of the two specie system and the bulk density ρ are defined by

$$u = \frac{\rho_s u_s + \rho_w u_w}{\rho}; \quad p = p_s + \rho_w$$

Using these definitions, dividing equation (2.1) by Δx and taking the limit as $\Delta x \to 0$, one has

$$-\frac{d}{dx} \int_{-h(x)/2}^{+h(x)/2} \rho u dy + N(x) + F_w = 0. \qquad (2.2)$$

The bulk fluid density is related to the solute molar concentration C_s by

$$\rho = (M_s - \frac{\bar{V}_s}{\bar{V}_w} M_w) C_s + \frac{M_w}{\bar{V}_w}$$

where M is the molecular weight and V the specific molar volume. With typical solute concentrations for the biological systems considered on the order of 2×10^{-4} moles/cc the bulk fluid density is nearly independent of solute concentration. If an integral average velocity is defined as

$$u = \frac{1}{h(x)} \int_{-h(x)/2}^{+h(x)/2} u \, dy$$

and ρ assumed constant, the overall continuity equation can be written in terms of this integral property as:

$$\rho \frac{d(\bar{u}h)}{dx} = N(x) + F_w \qquad (2.3)$$

The passive water flux across an isothermal semi-permeable membrane separating two non-isotonic solute bathing solutions can be linearly related to the solute concentration difference across the membrane if the hydrostatic pressure differential across the membrane is not excessively large and if the bathing solutions contain dilute concentrations of solute. Both of these conditions are met in normal biological membranes. Equation (2.3) is therefore written as:

$$\rho \frac{d(uh)}{dx} = N(x) \, 2 \, P_w \, \delta C_s \qquad (2.4)$$

where P_w is a water permeability coefficient for the lateral membrane and $\delta C_s = C_{sw} - C_{so}$ is the local discontinuity in solute concentration across the intercellular membrane with C_{sw} and C_{so} being the solute concentrations at the membrane wall within the channel and in the cell interior, in that order.

2 (b) Conservation of Solute Equation

The derivation of the solute conservation relation for the differential control volume closely parallels that just performed for total mass conservation. The counterpart of (2.2) is obtained by replacing ρu by the solute flux $\rho_s u_s$. Requiring $F_s = 0$ and taking the limit as $\Delta x \to 0$ one has

$$\frac{d}{dx} \int_{-h(x)/2}^{+h(x)/2} \rho_s u_s \, dy = N(x) \qquad (2.5)$$

The integrand of (2.5) can be represented as a sum of convective and diffusional solute fluxes by defining a diffusional streamwise solute flux J_{sx} relative to the mass average velocity u

$$J_{sx} = \rho_s (u_s - u).$$

Equation (2.5) then becomes:

$$\frac{d}{dx} \int_{-h(x)/2}^{+h(x)/2} M_s C_s u \, dy + \frac{d}{dx} \int_{-h(x)/2}^{+j(x)/2} J_{sx} dy = N(x) \qquad (2.6)$$

An integral average convective solute flux $\overline{C_s u}$ and an integral average streamwise diffusional flux $\overline{J_{sx}}$ are now defined as

$$\overline{C_s u} = \frac{1}{h} \int_{-h/2}^{+h/2} C_s u \, dy; \quad J_{sx} = \frac{1}{h} \int_{-h/2}^{+h/2} J_{sx} dy$$

If pressure diffusion effects are neglected, the local streamwise diffusional flux is linearly related to the streamwise solute concentration gradient by,

$$J_{sx} = M_s \frac{\rho_w}{\rho} D \frac{\partial C_s}{\partial x} \qquad (2.7)$$

Using the above definitions of the integral average properties, one can write the solute conservation equation (2.6) as

$$M_s \frac{d}{dx} \overline{(C_s u h)} + \frac{d}{dx} (\overline{J}_{sx} h) = N(x) \qquad (2.8)$$

2(c) Momentum Equation

An order of magnitude analysis of the steady state Navier-Stokes momentum equations shows that these equations can be approximated by those for a quasi-uni-directional flow field provided $\frac{\rho U_o h_o}{\mu} \alpha << 1$ and $\frac{h_o}{L} << 1$ where U_o is the characteristic streamwise velocity component, h_o and L are respectively the characteristic channel height and length, α is a characteristic streamline slope, and μ is the fluid viscosity. This condition is similar to that used in lubrication theory where the usual Reynolds number is modified to take into account the small streamline inclination at boundaries. In the present context α must be generalized to include the effect of passive water movement and secretion at the channel boundaries. The above conditions are satisfied under most circumstances for extracellular channel transport with the possible exception of regions in close proximity to stagnation points within the channel. One would expect such regions of deviation from unidirectional flow to be limited to axial distances of only several channel heights and, therefore, not to significantly affect the flow behavior on the larger length scale of the channel length L.

The momentum equation, therefore, requires that

$$\frac{\partial p}{\partial y} = 0 \qquad (2.9)$$

$$\frac{\partial p}{\partial x} = \mu \frac{\partial^2 u}{\partial y^2} \qquad (2.10)$$

From (2.9) $p = p(x)$ and (2.10) can be integrated across the channel to give

$$h(x) \frac{dp}{dx} = \mu \frac{\partial u}{\partial y} \Bigg|_{y = -h/2}^{y = +h/2} \tag{2.11}$$

where the right-hand side represents the shear stress at the upper and lower lateral boundaries.

2(d) Continuity of Flux at the Lateral Boundaries

The diffusional flux of salt which crosses the lateral boundaries of the channel must be consistent with the normal gradient of the solute concentration at these boundaries. Therefore at the lateral boundaries $y = \pm h/2$.

$$J_{sy} = - M_s \frac{\rho_w}{\rho} D \frac{\partial C_s}{\partial y} = \rho_s (v_s - v)$$

where v is the normal velocity component.

The second equality on the right can be written in terms of the total solute and water fluxes crossing the upper lateral membrane

$$\rho_s (v_s - v) = \frac{\rho_w}{\rho} \frac{N(x)}{2} - \frac{\rho_s}{\rho} \frac{F_w}{2}$$

Combining these two results and the definition of the passive water flux $F_w = 2P_w \delta C_s$, one obtains at the lateral boundary $y = + h/2$

$$2M_s D \frac{\partial C_s}{\partial y} = N(x) - \frac{M_s C_s}{\rho_w} p_w \delta C_s \tag{2.12}$$

2(e) Dimensionless Equations and Parameters

The four equations (2.4), (2.8), (2.11) and (2.12) constitute the basic conservation relations for the determination of the pressure, velocity and solute concentration in the channel. Additional qualitative insight into the behavior of these equations can be had by casting them in dimensionless

form and deducing the basic dimensionless groups that enter into the equations and boundary conditions. To this end all the variables in the problem are non-dimensionalized according to the following relations, the dimensionless variables being denoted by asterisks:

$$h^* = \frac{h}{h_o}, \quad x^* = \frac{x}{h_o}, \quad y^* = \frac{y}{h_o}$$

$$C_s^* = \frac{C_s}{C_{so}}, \quad u^* = \frac{u}{U_o}, \quad p^* = \frac{p}{p_o}, \quad N^* = \frac{N}{N_o} \tag{2.13}$$

The quantities h_o and N_o represent some arbitrarily specified reference channel height and active solute flux, respectively, and C_{so} is the concentration in the cell interior. The previously mentioned order of magnitude analysis of the momentum equation obviates the need to introduce separate x and y coordinate scalings. U_o and P_o are unknown and are to be determined by an appropriate balancing of terms in the governing equations. This non-dimensionalization procedure is equivalent to that performed for the D ξ B equations by Segel (1970). The only difference is that Segel uses a streamwise coordinate scaling based on the secretory site length in place of the channel height.

Substitution of the relations in (2.13) into equations (2.4). (2.8), (2.11) and (2.12) yields, after dividing by the coefficients of the first terms on the left hand side of the equations:

$$\frac{d(\bar{u}^* h^*)}{dx^*} = \frac{N_o}{\rho U_o} N^* + \frac{2P_w \rho_{so}}{M_s \rho U_o} (C_{sw}^* - 1) \tag{2.14}$$

$$\frac{d\ (\overline{C_s} u^* h^*)}{dx^*} + \frac{D}{h_o U_o} \frac{d(\overline{J_{sx}}^* h^*)}{dx^*} = \frac{N_o}{\rho_{so} U_o} N^* \tag{2.15}$$

$$2\left.\frac{\partial C_s^*}{\partial y^*}\right|_{y^* = \frac{h^*}{2}} = \frac{N_o h_o}{\rho_{so} D} N^* - \frac{P_w h_o \rho_{so}}{M_s D \rho} C_{sw}^* (C_{sw}^* - 1) \qquad (2.16)$$

$$h^* \frac{dp^*}{dx^*} = \frac{\mu U_o}{P_o h_o} \left.\frac{\partial u^*}{\partial y^*}\right|_{y = -\frac{h^*}{2}}^{y = \frac{h^*}{2}} \qquad (2.17)$$

where we have assumed that $\rho_w = \rho$, have let $\rho_{so} = C_{so} M_s$ and have defined the non-dimensional average quantities:

$$u^* = \frac{\bar{u}}{U_o}, \quad \overline{C_s u^*} = \frac{\overline{C_s u}}{C_{so} U_o}, \quad \overline{J_{sx}^*} = -\frac{1}{h^*} \int_{-h^*/2}^{h^*/2} \frac{\partial C_s}{\partial x^*} dx^* = \frac{h_o}{\rho_{so} D} \overline{J_{sx}}$$

The dimensionless equations (2.14) - (2.17) are seen to contain seven dimensionless coefficient groups involving the five characteristic reference quantities. The number of independent groups can be reduced by the proper choice of the yet unspecified reference quantities U_o and P_o. U_o is chosen so that the coefficient of the convective and diffusive terms in equations (2.15) are equal. Setting $U_o = D/h_o$ reduces the dimensionless coefficient of the diffusive term to unity and elminates one of the dimensionless groups. The choice for P_o is obvious since it appears in only one group. Setting P_o equal to $\mu U_o / h_o$ in equation (2.17) eliminates one more dimensionless coefficient and makes the coefficients of the left and right hand sides of the equation both equal to unity. The remaining five dimensionless coefficients can now be redefined in terms of the three groups,

$$\epsilon = \frac{\rho_{so}}{\rho}, \quad \eta = \frac{N_o h_o}{\rho D}, \quad \text{and} \quad R = \frac{P_w h_o}{M_s D}$$

Substitution of these quantities into equations (2.14) - (2.17) yields,

$$\frac{d(\bar{u}^* h^*)}{dx^*} = \eta N^* + 2\epsilon R(C_{sw}^* - 1) \qquad (2.18)$$

$$\frac{d}{dx^*}\left(\overline{C_s u^* h^*}\right) + \frac{d}{dx^*}\left(\overline{J}^*_{sx} h^*\right) = \frac{\eta}{\varepsilon} N^* \tag{2.19}$$

$$2 \left.\frac{\partial C_s^*}{\partial y^*}\right|_{y^* = h^*/2} = \frac{\eta}{\varepsilon} N^* - \varepsilon R C^*_{sw} \left(C^*_{sw} - 1\right) \tag{2.20}$$

$$h^* \frac{dp^*}{dx^*} = \left.\frac{\partial u^*}{\partial y^*}\right|_{y^* = -h^*/2}^{y^* = h^*/2} \tag{2.21}$$

The dimensionless group η represents the ratio of the active transport flux of solute to the convective flux of water while R is a measure of the ratio of the passive flux of water across the lateral boundaries to the convective flux of solute. The third parameter ε is simply a measure of the solute concentration in the cell interior. The boundary conditions introduce five additional dimensionless groups, $C_s^*(0) = C_s(0)/C_{so}$, $C_s^*(L) = C_s(L)/C_{so}$ representing the solute concentration at the two ends of the channel; $L^* = L/h_o$ the dimensionless channel length; U(0), a dimensionless entrance velocity in an open geometry channel; and a dimensionless secretory site length $\Delta\ell/h_o$.

For a given channel, one specifies the values for h_o, L, D, P_w, ρ, ρ_s and M_s and, thereby, the values of η and R. In a closed geometry channel, where the mass flux and axial solute concentration gradient both vanish at the closed end, only $C_s^*(L)$ or $C_s^*(0)$ remains as a free parameter to satisfy the boundary value problem. For open geometry channels, three degrees of freedom, $U^*(0)$, $C_s^*(0)$ are available to satisfy end conditions for solute concentration and hydrodynamic pressure differential.

2 (f) Velocity and Concentration Profiles

Equations (2.18) through (2.21) permit one to define at most three profile coefficients for the description of the velocity and solute concentration

fields. The fourth unknown function of x is the pressure. If one assumes that the passive water flux produces only small departures from the no slip boundary condition at the lateral boundaries and that the fluid viscosity is uniform across the channel, the previously mentioned order of magnitude analysis of the Navier-Stokes momentum equation suggests that a one parameter Poiseuille like parabolic velocity profile is appropriate for the extracellular channel flow. It is assumed, therefore, that the velocity profile is of the form:

$$u^*(x, y) = U_m^* \left[1 - \left(\frac{2y^*}{h^*}\right)^2\right]$$

This profile family satisfies equations (2.9), (2.10), the no slip boundary condition and allows the centerline velocity U_m and hence the bulk flow to vary as a function of x.

For the solute concentration profile a two parameter family was selected in terms of the dimensionless concentration C^*_{sw} at the lateral boundary and the centerline concentration C^*_{sm}. This permits an estimate of the rate of mixing across the channel and provides an independent measure of the local osmotic effect along the lateral boundary. A convenient profile that allows two parameters C^*_{sw} and C^*_{sm} to vary in a continuous manner along the channel is the quadratic form

$$C^*_s = C^*_{sw} + (C^*_{sm} - C_{sw}) \left[1 - \frac{2y^*}{h^*})^2\right]$$

2(g) Equations for the Profile Coefficients and Pressure

The dimensionless integral average properties can now be expressed in terms of the three profile coefficients introduced in the last subsection as follows:

$$\bar{u}^* = \frac{2}{h^*} \int_o^{h^*/2} u^* \, dy^* = \frac{2}{3} U_m^* (x)$$

$$\overline{C_s u^*} = \frac{2}{h^*} \int_0^{h^*/2} (C_s^* u^* \, dy) = \frac{6}{5} U_m^* C_{sw}^* - \frac{8}{15} U_m^* C_{sm}^*$$

$$J_{sx} = -\left(\frac{2}{3} \frac{dC_{sm}^*}{dx^*} + \frac{1}{3} \frac{dC_{sw}^*}{dx^*}\right)$$

Substitution of these expressions into equations (2.18) through (2.21) yields with the asterisk omitted

$$\frac{2}{3} \frac{d(U_m h)}{dx} = \eta N + 2\varepsilon R(C_{sw} - 1) \tag{2.22}$$

$$\frac{6}{5} \frac{d}{dx}(U_m C_{sw} h) - \frac{8}{15} \frac{d}{dx}(U_m C_{sm} h) - \frac{d}{dx}\left(\frac{2}{3} h \frac{dC_{sm}}{dx} + \frac{1}{3} h \frac{dC_{sw}}{dx}\right) = \frac{\eta}{\varepsilon} N \tag{2.23}$$

$$\frac{8}{h}(C_{sw} - C_{sm}) = \frac{\eta}{\varepsilon} N - \varepsilon R C_{sw}(C_{sw} - 1) \tag{2.24}$$

$$\frac{dp}{dx} = -8 \frac{U_m}{h^2} \tag{2.25}$$

In presenting the results it will be convenient to refer to the dimensionless volume flux Q* at any station rather than U_m and to introduce a dimensionless total solute flux Q_s^*. From the three expressions for the integral average properties above

$$Q^* = \int_{-h^*/2}^{h^*/2} u^* \, dy^* = \frac{2}{3} U_m^*(x) \, h^*(x) \tag{2.26a}$$

and

$$Q_s^* = \bar{J}_{sx}^* h^* + \overline{C_s u^*} h^* = U_m^* h^* \left(\frac{6}{5} C_{sw}^* - \frac{8}{15} C_{sm}^*\right) - h^*\left(\frac{2}{3} \frac{dC_{sm}^*}{dx^*} + \frac{1}{3} \frac{dC_{sw}^*}{dx^*}\right) \tag{2.26b}$$

where again the asterisk will be dropped in future use.

3. Approximate Analytic Solutions

Equations (2.22), (2.23), (2.24) and (2.25) provide a coupled system of one algebraic and three ordinary differential equations for the three profile coefficients C_{sm}, C_{sw}, U_m and the pressure. Numerical solutions to varied split end point boundary value problems associated with these four equations are presented in sections 5 and 6. Our objective here is to see if approximate analytic solutions can be obtained for physiologically meaningful simplifications to the system (2.22) - (2.25). To this end, one notes that for the extracellular channels in the ciliary body epithelium both η and R are of order 10^{-3} or smaller based on the best available estimates of the quantities comprising these dimensionless coefficients. For these conditions the right hand side of (2.24) $\ll 1$ and $C_{sw} \approx C_{sm}$. Thus, the necessary conditions for the validity of the instantaneous mixing hypothesis used in Diamond and Bossert, which assumes a uniform concentration profile across the channel with $C_s = C_{sw} = C_{sm}$ is that $\frac{\eta}{\varepsilon}$ and $\varepsilon R \ll 1$. This hypothesis is reasonable for the ciliary body and the gall bladder, but probably not valid for short extracellular channels such as the intracellular canaliculi of the small intestine.

Two additional simplifications that greatly reduce the difficulty of the analysis without altering the basic physics are to let the channel height be constant h = 1 and to treat the active transport site as a point rather than a distributed solute source. If this source is located at $x = L_s$, then for $x \lesseqgtr L_s$ equations (2.22), (2.23) and (2.25) reduce to

$$\frac{d}{dx}(QC_s) - \frac{d^2C_s}{dx^2} = 0 \qquad (3.1)$$

$$\frac{dQ}{dx} = 2\varepsilon R\,(C_s - 1) \qquad (3.2)$$

$$\frac{dP}{dx} = -12Q \qquad (3.3)$$

while the source strength S is defined by

$$S = \int_{L_s^-}^{L_s^+} \frac{\eta}{\epsilon} N dx \tag{3.4}$$

where $L_s^- \to L_s^+$. The matching conditions at the solute source are

$$P(L_s^+) = P(L_s^-) \tag{3.5a}$$

$$C_s(L_s^+) = C_s(L_s^-) \tag{3.5b}$$

$$Q(L_s^+) - Q(L_s^-) = \epsilon S \tag{3.5c}$$

$$\frac{dC_s}{dx}(L_s^+) - \frac{dC_s}{dx}(L_s^-) = -S + \epsilon S C_s(L_s) \tag{3.5d}$$

where the last two conditions are obtained by integrating equations (2.22) and (2.23) across the secretory site and then applying the limiting process $L_s^- \to L_s^+$ for a point source. One observes from (3.5d) that the secretory site produces a discontinuity in concentration gradient at the source location whose magnitude to lowest order is proportional to the source strength.

The boundary conditions at the channel entrance and exit are:

$$C_s(0) = C(0) \tag{3.5e}$$

$$C_s(L) - C_s(0) = \Delta C \tag{3.5f}$$

$$P(L) - P(0) = \Delta P \tag{3.5g}$$

$$P = P(0) \text{ at } x = 0 \tag{3.5h}$$

where $C(0)$, ΔC, $P(0)$ and ΔP are prescribed.

The simplified system of equations (3.1) - (3.3) is still not easy to solve because of the non-linear coupling between Q and C_s. This last difficulty can be handled by making use of the fact that in the ciliary body, $\epsilon R \ll 1$ and that the transport mechanisms are insensitive to the overall pressure level in the channel; the driving force is ΔP. We therefore develop

C_s, Q and P as a double perturbation expansion in integer powers ϵR and ΔP. This expansion has the effect of separating out, to first order the convective corrections for the filtration flow produced by the externally applied pressure differential ΔP and the passive water movement across the lateral boundaries due to local osmosis.

$$\begin{aligned} C_s &= C^{(o)} + \epsilon R C_1^{(1)} + \Delta P C_2^{(1)} + \cdots \\ Q &= Q^{(o)} + \epsilon R Q_1^{(1)} + \Delta P Q_2^{(1)} + \cdots \\ P &= P^{(o)} + \epsilon R P_1^{(1)} + \Delta P P_2^{(1)} + \cdots \end{aligned} \tag{3.6}$$

The series solutions denoted by (3.6) will not in general be uniformly valid for large x unless the independent variable x is strained. This complication occurs because the range of the x integration, which is the channel length L, is $>> 1$ and can give rise to first order convective corrections $\epsilon R C_1^{(1)}$ and $\Delta P C_2^{(1)}$ which can be of the same order or larger than $C^{(o)}$. Inspection of (3.1), (3.2), (3.3) shows that such secular behavior can be anticipated if either Q which is of order ϵRL is $\geq 0(1)$. To avoid this undesirable growth of the solution (3.6) for $x >> 1$ we introduce a two parameter PLK type coordinate expansion.

$$x = x_o + \epsilon R x_1(x_o) + \Delta P x_2(x_o) + \cdots \tag{3.7}$$

The unknown functions $C_i^{(j)}$, $Q_i^{(j)}$ and $P_i^{(j)}$ appearing in (3.6) are now considered as functions of the strained coordinate x_o and are obtained by solving the differential equations which obtain when (3.6) and (3.7) are substituted into (3.1), (3.2) and (3.3) and coefficients of like order in ϵR and ΔP are equated.

To zeroth order:

$$\frac{dp^{(o)}}{dx_o} = -12Q^{(o)} \tag{3.8a}$$

$$\frac{d}{dx_o}\left(Q^{(o)}C^{(o)}\right) - \frac{d^2C^{(o)}}{dx_o^2} = 0 \tag{3.8b}$$

$$\frac{dQ^{(o)}}{dx_o} = 0 \tag{3.8c}$$

To first order in εR:

$$\frac{dP_1^{(1)}}{dx_o} - \frac{dx_1}{dx_o}\frac{dP^{(o)}}{dx_o} = -12Q_1^{(1)} \tag{3.9a}$$

$$\frac{d^2}{dx_o^2}C_1^{(1)} = \frac{d}{dx_o}\left[Q^{(o)}C_1^{(1)} + Q_1^{(1)}C^{(o)}\right] - \frac{dx_1}{dx_o}\frac{d}{dx_o}\left[Q^{(o)}C^{(o)}\right] + 2\frac{dx_1}{dx_o}\frac{d^2C^{(o)}}{dx_o^2} + \frac{d^2x_1}{dx_o^2}\frac{dC^{(o)}}{dx_o} \tag{3.9b}$$

$$\frac{d}{dx_o}Q_1^{(1)} - \frac{dx_1}{dx_o}\frac{dQ^{(o)}}{dx_o} = 2\left(C^{(o)}-1\right. \tag{3.9c}$$

To first order in ΔP:

$$\frac{dP_2^{(1)}}{dx_o} - \frac{dx_2}{dx_o}\frac{dP^{(o)}}{dx_0} = -12Q_2^{(1)} \tag{3.10a}$$

$$\frac{d^2C_2^{(1)}}{dx_o^2} = \frac{d}{dx_o}\left[Q^{(o)}C_2^{(1)} + Q_2(1)C^{(o)}\right] - \frac{dx_2}{dx_o}\frac{d}{dx_o}\left[Q^{(o)}C^{(o)}\right] + 2\frac{dx_2}{dx_o}\frac{d^2C^{(o)}}{dx_o^2} + \frac{d^2x_2}{dX_o^2}\frac{dC^{(o)}}{dx_o} \tag{3.10b}$$

$$\frac{d}{dx_o}Q_2^{(1)} - \frac{dx_2}{dx_o}\frac{d}{dx_o}Q^{(o)} = 0 \tag{3.10c}$$

Equations (3.8), (3.9), (3.10) each constitute a system of six ordinary differential equations; three for the range $0 < x < L_s$ and three for the range $L_s < x < L$; whose total order is eight. The eight unknown inegration constants are determined for each order system by the eight

boundary and matching conditions that are obtained by substituting (3.6) and (3.7) into (3.5) and equating coefficients of each power of εR and ΔP. The boundary conditions for the lowest order set of equations (3.8) are homogeneous for P and inhomogeneous for C_s, while for the first order set (3.9) the boundary conditions on both P and C_s are homogeneous. For the first order set (3.10) the pressure boundary condition is inhomogeneous since it introduces the filtration pressure differential ΔP. With this ordering the total contributions to the water flux Q from osmosis, active transport and filtration can be of comparable magnitude.

For each higher order system one has to solve an auxiliary second order differential equation for the coordinate straining functions x_i in the two regions $0 < x < L_s$ and $L_s < x < L$. The differential equations for x_1 and x_2 are determined by suppressing the undesirable growth that results from the inhomogeneous terms in (3.9b) and (3.10b). These terms lead to solutions for $C_1^{(1)}$ and $C_2^{(1)}$ which exhibit a monatonically increasing algebraic growth for values of $x >> 1$ and consequently a divergence of the series (3.6) for large x. To suppress this secular behavior one requires instead that $C_1^{(1)}$ and $C_2^{(1)}$ satisfy the homogeneous equations.

$$\frac{d^2C_1^{(1)}}{dx_o^2} = 0; \quad \frac{d^2C_2}{dx_o^2} = 0 \text{ for } \begin{matrix} 0 < x_o < L_{os} \\ L_{os} < x_o < L_o \end{matrix} \qquad (3.11a)$$

that obtain by letting the unknown functions x_1 and x_2 in (3.9b) and (3.10) obey

$$\frac{d^2x_{1,2}}{dx_o^2}\frac{dC^{(o)}}{dx_o} + \frac{dx_{1,2}}{dx_o}\left[2\frac{d^2C^{(o)}}{dx_o^2} - \frac{d}{dx_o}Q^{(o)}C^{(o)}\right]$$

$$+ \frac{d}{dx_o}\left[Q^{(o)}C_{1,2}^{(1)} + Q_{1,2}^{(1)}C^{(o)}\right] = 0 \tag{3.11b}$$

where L_o represents the location of the channel exit in the x_o coordinate. The boundary and matching conditions for the unknown functions x_1 and x_2 are to some extent arbitrary. At $x_o = L_{os}$, the source location in the strained coordinate system, it is reasonable to require that the strained coordinate be continuous and that the compatibility condition (3.5d) be satisfied to first order in εR and ΔP:

$$x_1(L_{os}^-) = x_1(L_{os}^+);\ x_2(L_{os}^-) = x_2(L_{os}^+) \tag{3.12a}$$

$$\left|\frac{dC_1^{(1)}}{dx_o} - \frac{dx_1}{dx_o}\frac{dC^{(o)}}{dx_o}\right|_{x_o = L_{os}^+} = \left|\frac{dC_1^{(1)}}{dx_o} - \frac{dx_1}{dx_o}\frac{dC^{(o)}}{dx_o}\right|_{x_o = L_{os}^-} + \frac{S}{R}C^{(o)}(L_{os}) \tag{3.12b}$$

$$\left|\frac{dC_2^{(1)}}{dx_o} - \frac{dx_2}{dx_o}\frac{dC^{(o)}}{dx_o}\right|_{x_o = L_{os}^+} = \left|\frac{dC_2}{dx_o} - \frac{dx_2}{dx_o}\frac{dC^{(o)}}{dx_o}\right|_{x_o = L_{os}^-} \tag{3.12c}$$

Equations (3.11b) are of second order and thus permit the specification of two additional conditions. For compatability with (3.2) and (3.5b) one must require

$$\left.\frac{dx_1}{dx_o}\right|_{x_o = L_{os}^-} = \left.\frac{dx_1}{dx_o}\right|_{x_o = L_{os}^+};\quad \left.\frac{dx_2}{dx_o}\right|_{x_o = L_{os}^-} = \left.\frac{dx_2}{dx_o}\right|_{x_o = L_{os}^+} \tag{3.12d}$$

and for convenience we choose

$$x_1(o) = x_2(o) = 0 \tag{3.12e}$$

For $C_1^{(1)}$ and $C_2^{(1)}$ to be zero for all x_o and satisfy (3.11a), $C_1^{(1)}$ and $C_2^{(1)}$ must obey homogeneous boundary and matching conditions. The first order conditions derived from (3.5b, e and f) and (3.12b and e) will satisfy this requirement provided

$$\left.\frac{dC_{1,2}^{(1)}}{dx_o}\right|_{x_o = L_{os}^-} = \left.\frac{dC_{1,2}^{(1)}}{dx_o}\right|_{x_o = L_{os}^+}$$

in (3.12b and c). In this manner the undesireable growth of the dependent variables is eliminated through the coordinate straining functions. With the conditions (3.12) one is not free to specify the values of x_o at the secretory site and at the channel exit. These are determined from a solution of the two simultaneous equations which obtain when $x = L_s$ and $x = L$ in (3.7). These equations, which are implicit algebraic relations for L_{os} and L_o must be solved numerically.

The zeroth order volume flux gradient $dQ^{(o)}/dx_o$ vanishes by (3.8c) and the zeroth order pressure gradient $dP^{(o)}/dx_o$ vanishes after solving (3.8a and c) with appropriate boundary conditions. The first order pressure and volume flux gradients in (3.9a and c) and (3.10a and c) are then indpendent of the coordinate straining as represented by dx_1/dx_o and dx_2/dx_o and depend only on the zeroth order concentration solution. The coordinate straining does enter into the second order flux corrections

$Q_{1,2}^{(2)}$ and pressure corrections $P_{1,2}^{(2)}$ which are derived from (3.2) and (3.3)

To order $(\varepsilon R)^2$ and $(\Delta P)^2$

$$\frac{dQ_{1,2}^{(2)}}{dx_o} = \frac{dQ_{1,2}^{(1)}}{dx_o}\ \frac{dx_{1,2}}{dx_o}\ ;\quad \frac{dP_{1,2}^{(2)}}{dx_o} = -12Q_{1,2} + \frac{dP_{1,2}^{(1)}}{dx_o}\ \frac{dx_{1,2}}{dx_o} \tag{3.13}$$

(a) Zeroth order solution

The solution of equations (3.8) and associated boundary and matching conditions is

$$P^{(o)} = P(o) \tag{3.14a}$$

$$Q^{(o)} = 0 \tag{3.14b}$$

$$C^{(o)} = \left(\frac{\Delta C}{L_o} + \left(1 - \frac{L_{os}}{L_o}\ S\right)x_o + C(o) \qquad 0 < x_o < L_{os} \tag{3.14c}$$

$$C^{(o)} = \left(\frac{\Delta C}{L_o} - \frac{L_{os}}{L_o}\ S\right)x_o + C(o) + SL_{os} \quad L_{os} < x_o < L_o \tag{3.14d}$$

The lowest order solution thus involves no convective transport. This solution is simply a linear variation in concentration due to solute diffusion between two specified end states with a discontinuity in solute concentration gradient at the secretory site location $x_o = L_{os}$ whose magnitude is proportional to the source strength S. This basic behavior is clearly suggested by the curves in Figure 8.

(b) First order solution in εR

To solve equations (3.9) one first integrates (3.9c) for $x_o \lessgtr L_{os}$ using (3.14). The integration constants in the resulting expressions for $Q_1^{(1)}$ can not be evaluated directly since they are related to the pressure boundary conditions. The expressions for $Q_1^{(1)}$ are therefore substituted in (3.9a). The integral of (3.9a) leads to two relations for $P_1^{(1)}$ valid for $x_o \lessgtr L_{os}$ with four unknown constants. The latter are evaluated by applying the four appropriate first order boundary and matching conditions that are derived from (3.5a), (3.5c), (3.5g) and (3.5h). The desired expressions for $Q_1^{(1)}$ and $P_1^{(1)}$ valid in each region are:

$$Q_1^{(1)} = \alpha_1 x_o^2 + 2(C(o)-1)x_o + \alpha_3 \qquad o < x_o < L_{os} \qquad (3.15a)$$

$$Q_1^{(1)} = \alpha_\alpha x_o^2 + 2(C(o)+SL_{os}-1) + \alpha_4 \qquad L_{os} < x_o < L_o \qquad (3.15b)$$

$$P_1^{(1)} = -12[\frac{\alpha 1}{3} x_o^3 + (C(o)-1)x_o^2 + \alpha_3 x_o] \qquad o < x_o < L_{os} \qquad (3.15c)$$

$$P_1^{(1)} = -12[\frac{\alpha 2}{3} x_o^3 + (C(o)+SL_{os}-1)x_o^2 + \alpha_4 x_o] \qquad L_{os} < x_o < L_o \qquad (3.15d)$$

where

$$\alpha_1 = \frac{\Delta C}{L_o} + (1 - \frac{L_{os}}{L_o})S$$

$$\alpha_2 = \alpha_1 - S$$

$$\alpha_3 = -(1-\frac{L_{os}}{L_o})(\frac{S}{R} + \frac{1}{3} SL_{os}(2L_o - L_{os})) - (C(o) + \frac{\Delta C}{3} - 1)L_o$$

$$\alpha_4 = \alpha_3 + \frac{S}{R} - SL_{os}^2$$

Note that the first order boundary value problems for the pressure and water flux have been uncoupled from that for the concentration field. (3.15a) and (3.15b) are the first order approximations for the convective fluxes that would be produced in a channel with passive water movement due to local osmosis at its lateral boundaries and no transmembrane pressure on the lowest order solution for the concentration distribution (3.14). The pressure distribution (3.15c) and (3.15d) is the passively induced pressure field created by the local osmosis.

In view of (3.14b), (3.11b) reduces to an inhomogeneous second order differential equation for x_1 alone:

$$\frac{d^2x_1}{dx_o^2}\,\frac{dC^{(o)}}{dx_o} + \frac{d}{dx_o}\left(Q_1^{(1)}C^{(o)}\right) = 0 \qquad (3.16)$$

where $C^{(o)}$ and $Q_1^{(1)}$ are given by (3.14c, d) and (3.15a, b) respectively. The integration of (3.16) in the two regions $x_o \lessgtr L_{os}$ introduces a total of four unknown constants. These constants are evaluated by applying the four first order boundary and matching conditions associated with (3.12). The final results are:

$$x_1 = \frac{\alpha 5}{\alpha_1}x_o - \frac{\alpha_1}{4}x_o^4 - \left(C(o) - \frac{2}{3}\right)x_o^3 - \left(\frac{2C(o)(C(o)-1)}{\alpha_1} + \alpha_3\right)\frac{x_o^2}{2}$$

$$- \frac{\alpha_3 C(o)}{\alpha_1}x_o \qquad o < x_o < L_{os} \qquad (3.17a)$$

$$x_1 = \frac{\alpha_5}{\alpha_2}x_o - \frac{\alpha_2}{4}x_o^4 - \left(C(o)+SL_{os}-2/3\right)x_o^3 -$$

$$\left(\frac{2(C(o)+SL_{os})(C(o)+SL_{os}-1)}{} + \alpha_4\right)\frac{X_o 2}{2} - \frac{\alpha_4(C(o)+SL_{os})}{\alpha_2}x_o - \alpha_6 \qquad (3.17b)$$

$$L_{os} < x_o < L_o$$

where

$$\alpha_5 = \frac{1}{\alpha_2 - \alpha_1}\ \{-\alpha_1\alpha_2(SL_{os}^3 + \frac{S}{R}L_{os}) + [2\alpha_2 C(o)(C(o)-1) - 2\alpha_1(C(o) + SL_{os})$$
$$(C(o) + SL_{os} - 1)]\ L_{os}$$
$$+ \alpha_2\alpha_3 C(o) - \alpha_1\alpha_4(C(o) + SL_{os})\}$$

$$\alpha_6 = \alpha_5 L_{os}(\frac{\alpha_1 - \alpha_2}{\alpha_1\alpha_2}) - \frac{SL_{os}^4}{4} + [\frac{2C(o)(C(o)-1)}{\alpha_1} - \frac{2(C(o)+SL_{os})(C(o)+SL_{os}-1)}{\alpha_2}$$
$$-\frac{S}{R}]\ \frac{L_{os}^2}{2} + [\frac{\alpha_3 C(o)}{\alpha_1} - \frac{\alpha_4(C(o)+SL_{os})}{\alpha_2}]L_{os}$$

(c) First order solution in ΔP

The solutions to (3.10) are obtained in a manner exactly analogous to that used to obtain the results in part (b) above. After integration and application of appropriate boundary and matching conditions one obtains

$$Q_2^{(1)} = -\frac{1}{12L_o} \tag{3.18a}$$

$$P_2^{(1)} = -\frac{x_o}{L_o} \tag{3.18b}$$

The straining function is found to be

$$x_2 = \frac{\alpha_7}{\alpha_1}x_o + \frac{1}{12L_o}(\frac{x_o^2}{2} + \frac{C(o)}{\alpha_1}x_o) \qquad o < x_o < L_{os} \tag{3.19a}$$

$$x_2 = \frac{\alpha_7}{\alpha_2}x_o + \frac{1}{12L_o}(\frac{x_o^2}{2} + \frac{C(o)+SL_{os}}{\alpha_2}x_o) + \alpha_8 \qquad L_{os} < x_o < L_o \tag{3.19b}$$

where

$$\alpha_7 = \frac{\alpha_1(C(o)+SL_{os}) - \alpha_2 C(o)}{12L_o(\alpha_2 - \alpha_1)}$$

$$\alpha_8 = \alpha_7 L_{os}(\frac{\alpha_2 - \alpha_1}{\alpha_1\alpha_2}) + \frac{1}{12L_o}[\frac{C(o)}{\alpha_1} - \frac{C(o)+SL_{os}}{\alpha_2}]L_{os}$$

The second order solutions in $(\epsilon R)^2$ are obtained by using the results (3.15) and (3.17) in (3.13) and applying the appropriate second order boundary and matching conditions from (3.5). The detailed results are contained in the Appendix.

The approximate analytic solutions given above will be compared with the exact solutions of (2.22) through (2.25) in section 5 for the condition in which $\Delta P = 0$.

4. Results for Closed Extracellular Channels

The boundary value problem for extracellular channels with impermeable junctional complexes at the lumenal end $x = 0$, for example the gall bladder geometry shown in figure 1, is readily converted into an initial value problem in which equations (2.22), (2.23) and (2.25) are integrated numerically. C_{sm} and its derivatives are related to C_{sw} and its derivatives by the algebraic relation (2.24). Since $U_m(0) = 0$, $\frac{dC_{sw}(o)}{dx} = 0$ and the intial reference pressure is arbitrary, only one initial condition, the dimensionless initial concentration $C_{sw}(0)$ is left unspecified. In both D & B and Segel (1970) $C_{sw}(0)$ is uniquely determined by requiring that $C_{sw} = 1$. However, for reasons stated earlier this isotonic exit condition is an artificial one. $C_{sw}(L)$ can have any value depending on the mixing process that ensues between the channel effluent and the outer bathing solution. The boundary condition to determine $C_{sw}(0)$ is more properly applied at infinity where the solution is collected and the concentration uniform. This equilibrium concentration is given by $C_\infty = \frac{Q_s}{Q}$.

To examine the entire spectrum of possible behavior $C_{sw}(0)$ shall be treated as a free parameter in the present study. In particular we shall want to see if it possible within the framework of the local standing

gradient osmotic model as presently formulated to have both a channel concentration which is hypotonic relative to the cell interior solution and a vanishing concentration gradient at the exit station. As discussed in the introduction, both conditions would appear necessary if the water in the cell interior is to be replenished from the lumen and yet have the channel effluent and outer bathing solution both be isotonic relative to the lumenal fluid .

The unexpected result in figure 5 a is that concentration in the channel does not automatically relax to the concentration in the cell interior as the perfusion length for passive water movement increases. One observes that there is only one initial solute concentration C_{cr} at x= 0 that permits C_{sw} to asymptotically approach unity with vanishing gradient at large values of x. The dashed curve in figure 5 representing this unique solution curve separates two families of solutions with distinctly different behavior. For $C_{sw}(0) > C_{cr}$, curves 1 through 3 in figure 5 a, C_{sw} eventually grows without bound for large values of x and leads to a monotonically increasing water flux in the channel. For $C_{sw}(0) < C_{cr}$, curves 4 and 5 in figure 5a, C_{sw} decays monotonically towards zero for increasing values of x. Once $C_{sw} < 1.0$ water diffuses back into the cell interior and a reversal in flow direction will occur if the channel is sufficiently long, as depicted in curve 5 of figure 5b. One notes from figure 5 that only solutions of the type of curves 4 and 5 are possible if the exit boundary condition $C_{sw}(L) = 1$ is imposed as in D ξ B and Segel. The solution curves for other values of η, ϵ and R in the range of interest for epithelial membranes all exhibit the same qualitative behavior as shown in figure 5. Varying these dimensionless groups simply alters the value for C_{cr} and changes the decay rate of the neutral (dashed) curve.

We next wish to interpret these results in the context of

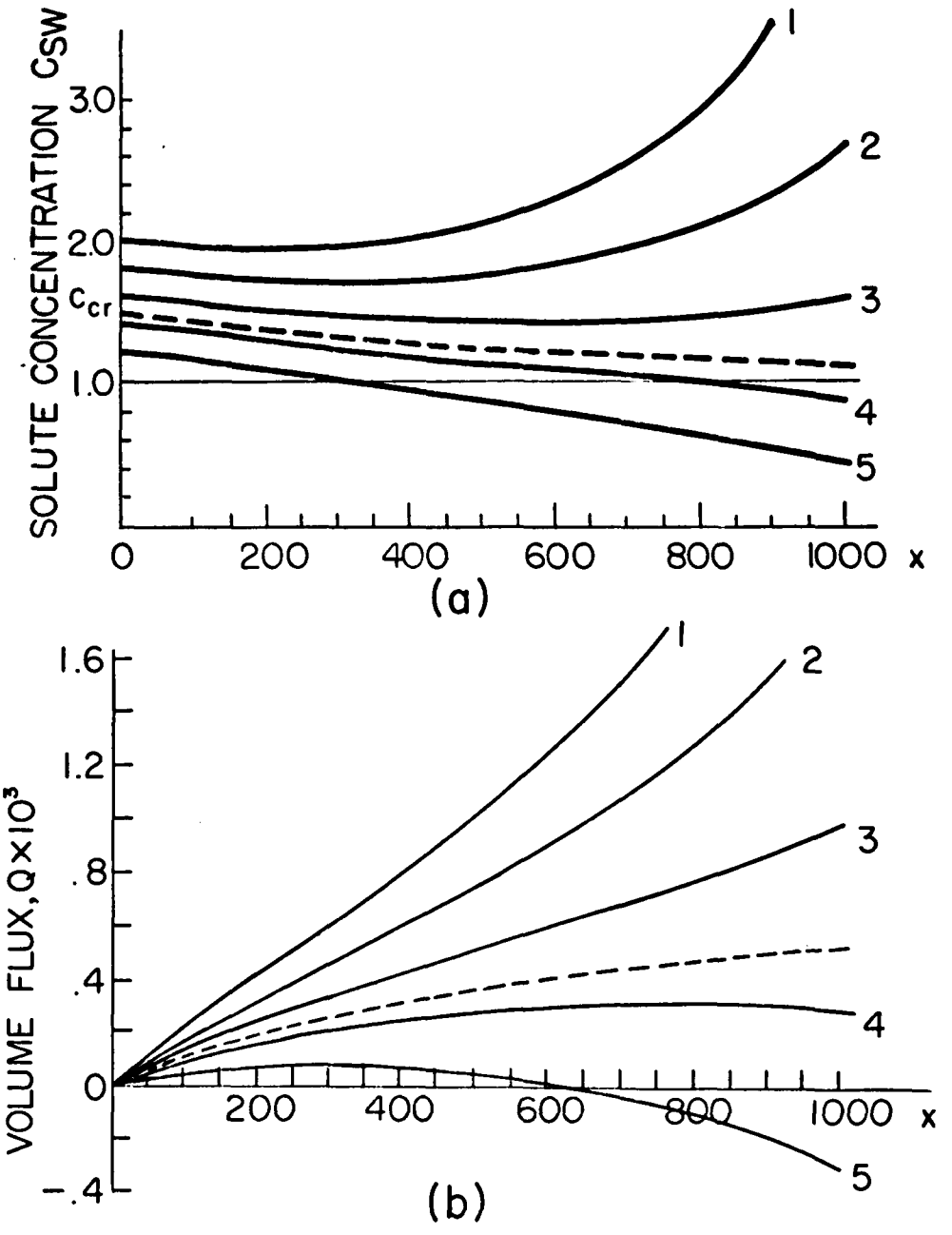

Figure 5. Effect of $C_{sw}(0)$ on The Distribution of Solute Concentration (a) and Volume Flux (b) in a Closed Extracellular Channel with Secretory Site Located between $0 < X < 50$; $\epsilon = .872 \times 10^{-2}$, $\eta = .135 \times 10^{-6}$, $R = .116 \times 10^{-3}$.

Diamond's (1964) experiments. If the effluent is to be isotonic with a well stirred outer bathing solution whose dimensionless far field concentration is C_∞ then the channel flow must reach the exit with both $C_{sw}(L) = C_\infty$ and $\frac{dC_{sw}(L)}{dx} = 0$ or further mixing would ensue at the channel exit. It is evident from figure 5a that when $C_{sw}(L) = C_\infty = 1$ only the dashed curve for the infinitely long channel satisfies both exit boundary conditions. Other solutions with a vanishing gradient at the channel exit are possible for finite length channels. These solutions are represented by the curves of the upper faminly in figure 5a where the channel exit is located at the minima, $\frac{dC_{sw}}{dx} = 0$. Thus, if L = 625 then curve 3 terminated at x = 625 would represent such a solution. These solutions all correspond to an outer bathing solution which is hypertonic relative to the cell interior, that is $C_\infty = C_{sw}(L) > 1$. No mention has yet been made of the concentration of the lumenal fluid. However, if the water in the cell interior is to be replenished from the lumen, as is widely assumed, then the lumenal fluid must be hypotonic relative to the cell interior. This is the basic paradox of the standing gradient model in explaining isotonic transport in the gall bladder. The solution in the cell interior, assuming homogeneity of cell water activity, obviously cannot at the same time be isotonic or hypotonic with the outer bathing solution and hypertonic with the lumenal solution of these two bathing solutions are isotonic. Also, there are no values of $C_{sw}(o)$ which allow the curves of the lower family in figure 4a to have a minimum where $C_{sw} < 1$. It would appear that basic modifications of the existing mathematical formulation are necessary if the conditions for both isotonic transport and water replenishment are to be explained using the local standing gradient osmotic concept for gall bladder epithelial transport. The solution curves in figure 5 may, however, be appropriate for other epithelia which produce hypertonic secretions.

The question as to how long a channel would be required for the channel flow to nearly equilibrate with the solution in the cell interior has been examined in detail in D ξ B and Segel (1970). While such equilibration ($C_{sw}(L) = 1$ and $\frac{dC_{sw}(L)}{dx} = 0$) cannot be exactly acheived for any finite length channel, these investigators have demonstrated that, provided the solution curves are of the type 4 or 5 in figure 5, the equilibration can be approached to within a few percent for estimated values of η, ϵ, R and L that are reasonable for gall bladder epithelium.

It is of interest to note that the curves in Fig. 5 may also represent the solutions to flow in channels which have an additional point solute source or sink located at a finite position downstream. All solutions of the lower family, represented typically by curves 4 and 5, eventually reach a zero concentration level with a negative, non-zero solute concentration gradient. Since negative concentrations are impossible, a discontinuity in the solute concentration gradient must be created at the point of zero concentration by a solute sink. The concentration then remains at zero beyond this point, since all of the solute has been removed from the channel by the sink. As the concentration decreases from that at station x= 0, the sink maintains a diffusional flux of salt sufficient to satisfy solute conservation requirements. Solutions of the upper family, typified by curves 1, 2 and 3 represent solutions for channels in which an additional solute source establishes a concentration level at a finite downstream location. At positions upstream of this source the net solute flux is constant and equal to that provided by the secretory site at the closed end. At downstream positions the net solute flux is increased by the contribution of the second source. This increase is achieved by a discontinuous reduction in the amount of back diffusion, i.e a reduction in the solute concentration gradient, at the source site. One

notes that solute concentration levels in general have an upper bound, equivalent to that for saturated, or supersaturated solutions.

5. Results for porous extracellular channels

The initial value problem for open and partially occluded extracellular channels with active transport is somewhat more difficult to handle numerically than the closed channel geometry just considered. In the case of channels completely occluded at one end both U_m and the concentration gradient $\frac{dC_{sw}}{dx}$ at the initial station are zero. Only the initial concentration $C_{sw}(0)$ is unknown. All three initial conditions are unknown in open channel systems. The two additional unknown initial conditions $U_m(0)$ and $\frac{dC_{sw}(0)}{dx}$ are related to the pressure difference $\Delta P = P(L) - P(0)$ and concentration difference $\Delta C_{sw} = C_{sw}(L) - C_{sw}(0)$ across the channel, see boundary conditions (3.5f, g). Thus, to integrate equations (2.22), (2.23) and (2.25) numerically trial values of $U_m(0)$ and $\frac{dC_{sw}(0)}{dx}$ had to be assumed and a variant of a steepest descent iteration routine used to satisfy the split end point boundary conditions on pressure and concentration. Solutions were assumed to have converged to the desired accuracy when the prescribed values of ΔP and ΔC_{sw} were satisfied to five significant digits.

To understand the essential features of the operation of an open channel with active transport and pressure filtration we first consider an idealized constant area channel with a secretory site centered symmetrically between the channel ends which are at the same concentration as the cell interior, see figure 6. Curves 1 a and b show the variation of dimensionless pressure P and volume flux Q when there is no applied pressure differential ΔP across the end stations. Water that enters the channel passively due to local osmosis divides at the center into two equal and

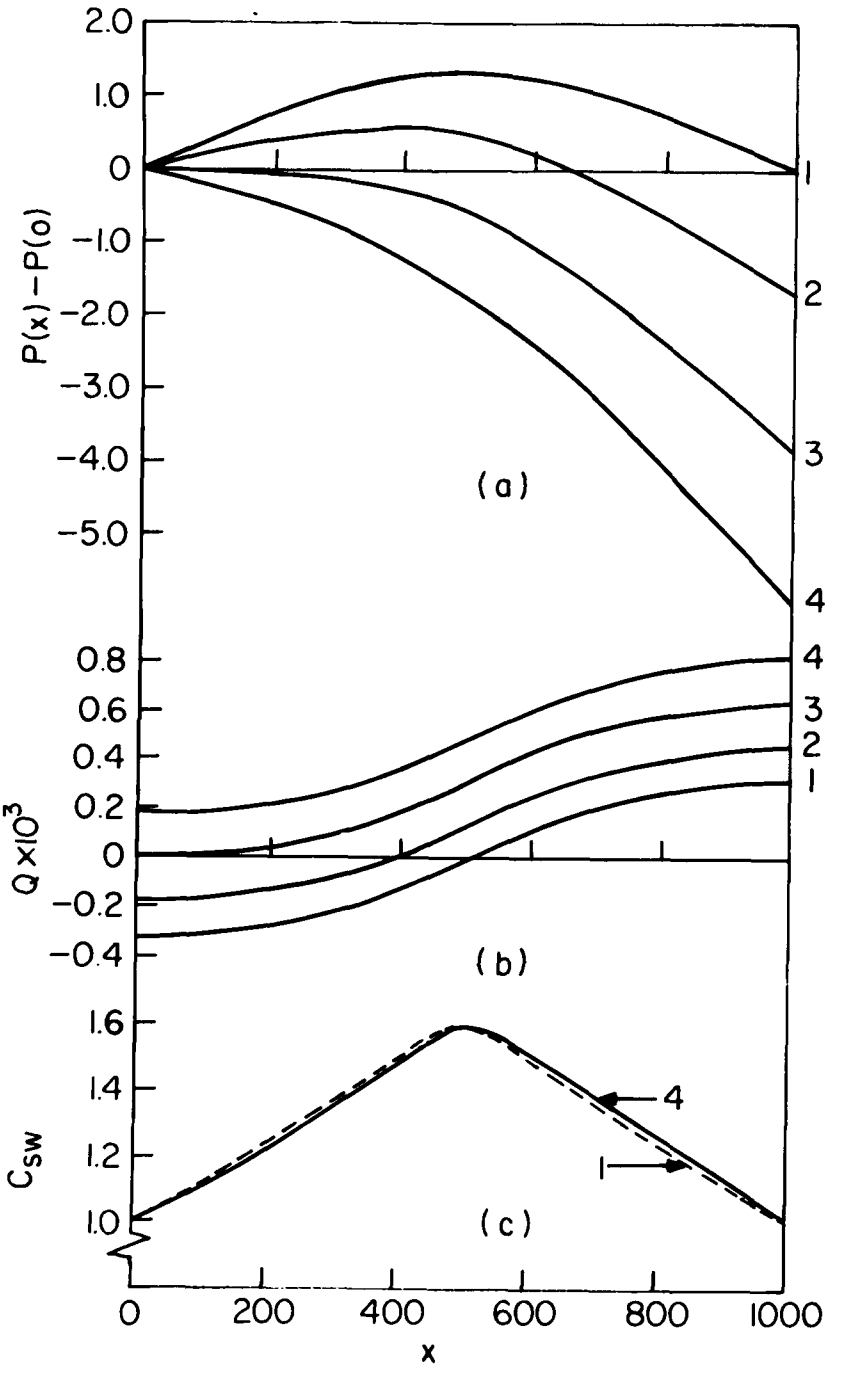

Figure 6. Effect of Pressure Filtration on the Distributions of Pressure (a), Volume Flux (b) and Solute Concentration (c) in an Open Geometry Channel with Secretory Site Located between $450 < X < 550$; $\epsilon = .872 \times 10^{-2}$, $\eta = .269 \times 10^{-6}$, $R = .116 \times 10^{-3}$, $C_{sw}(0) = C_{sw}(1000) = 1.0$

oppositely directed flows. Since both Q and the concentration gradient vanish because of symmetry at the channel center location, the flux conditions at the symmetry plane of the channel are the same as those at the initial station of a tight junction channel. Curves 2 a and b through 4 a and b show the effect of applying a monotonically increasing pressure differential across the membrane. An increase in the hydrodynamic pressure at the left end over that at the right, with $\Delta C_{sw} = 0$, will cause the locations at which $Q = 0$ to move to the left as shown in figure 6b. This location of the stagnation plane (i.e. $Q = 0$) is also the plane of maximum pressure, see equation (2.25). There is a critical applied pressure differential, curve 3 of figure 6 a when the filtration pressure is just sufficient to move the stagnation plane to the left end of the channel and thereby balance the water flux due to the local osmosis. Further increase in the applied pressure differential, (curves 4 a and b figure 6) results in unidirectional flow along the entire channel.

Figure 6 c shows the non-linear effect of convection on the streamwise concentration distribution produced by increasing the filtration pressure ΔP across the channel. Non-dimensional filtration pressures of 0(1) are typical of epithelial cell layers such as the ciliary body. The total passive water movement due to the local osmosis produced by the active transport is directly proportional to the total area under the concentration curve. One, therefore, concludes from figure 6 c that the concentration distribution is not significantly altered by convection and hence that the driving forces due to active transport and pressure filtration are essentially independent for epithelial cell layers. Thus, the channel efflux Q(L) is linearly related to ΔP and η, the dimensionless secretory site strength. This linear relation between membrane fluxes and driving forces is the fundamental simplifying hypothesis used in the irreversible thermodynamics theory of membrane transport and is also the basis for the perturbation expansions

(3.6) used herin. $C_1^{(1)}$ and $C_2^{(1)}$ in (3.6) can be viewed as the lowest order convective corrections to the linear theory.

Figure 7 shows the effect of varying the secretory site strength (value of η) on the movement of the stagnation plane for a symmetry channel. The $\eta = .269 \times 10^{-6}$ curve is obtained from the intersections with Q = 0 axis of the curves in figure 6b. Increasing the secretory site strength is equivalent to increasing the local osmotic effect and thus results in a smaller stagnation plane shift for a constant ΔP. The interesting feature of these curves is that the movement of the stagnation plane is a highly non-linear function of ΔP although, as just noted, epithelial membranes function in a region where all fluxes and driving forces are linearly related. The local value of Q(x) is linearly related to ΔP but unlike the flux at the channel exit Q(L) it is non-linear function of position since the local integrated area under the concentration curve and hence the local integrated passive water movement due to local osmosis varies non-linearly with position. The location of the stagnation plane is determined by the balance between the filtration flux and the integrated passive water movement due to local osmosis between the active transport site and the stagnation plane. On the other hand, the critical value of ΔP required to shift the stagnation plane to the channel entrance, the intersection of the curves in figure 7 with the ΔP axis, is almost linearly proportional to η. This is a result of the fact that the total area under the concentration curve, and hence the total local osmotic flux, is linearly independent of ΔP if the non-linear effects convection can be neglected.

Figure 8 a, b, c show the effect of applying an osmotic driving force ΔC_{sw} across a membrane with active transport, but no transmembrane pressure differential. The total passive water movement is the same for each set of curves and again the secretory site is located symmetrically

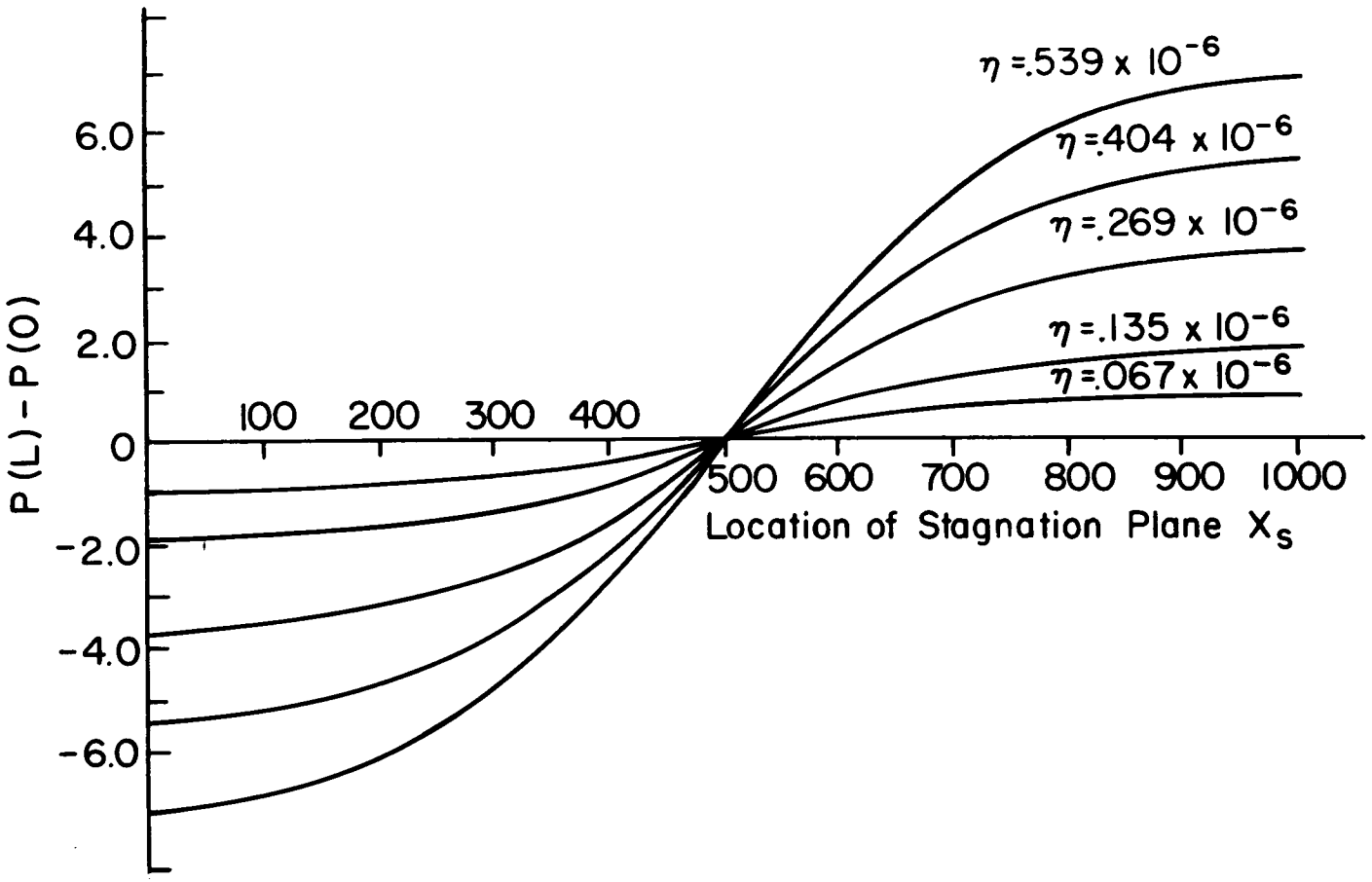

Figure 7. Effect of ΔP and η on the Shift of Stagnation Plane in an Open Geometry Channel with Secretory Site Located between $450 < X < 550$; $\epsilon = .872 \times 10^{-2}$, $R = .116 \times 10^{-3}$, $C_{sw}(0) = C_{sw}(1000) = 1.0$

between the end stations. These curves provide a convenient test as to the accuracy of the approximate analytical solutions presented in section 3. For the numerical solutions the secretory site had a finite length equal to two percent of the channel length whereas in the analytic solutions it is treated as a point source. The discontinuity in Q at the secretory site for the analytic curves is due to the active transport of salt and is the ϵS term in the matching condition (3.5c). The concentration curves in figure 8a show the nearly linear diffusion dominated behavior predicted by the lowest order analytic solutions (3.14c) and (3.14d). The analytic volume flux curves in figure 8b are the solutions (3.15a) and (3.15b) where the relationship between x and the strained coordinate x_o is obtained from (3.7), (3.17a) and (3.17b). The curves in figure 8c show the effect of an osmotic driving force on the pressure distribution in the channel with ΔP maintained at zero. The osmotic driving force has basically redistributed the flux Q(0) and Q(L) to the two end stations, while their sum is a constant since the total passive water movement is held fixed.

In figures 9a and b and 10 we examine the effect of secretory site location on the water and solute flux at the channel entrance and exit and on the concentration distribution in the channel. The only driving force is active transport. The total passive water movement into the channel is again held constant. Thus, the area under each of the curves in figure 10 is the same. The interesting behavior is that distribution of the solute fluxes to the two end stations is a much more sensitive function of secretory site location than the water fluxes.

The salt flux at the channel entrance exit depend principally on the diffusional gradient at the end stations established by the concentration profile and, therefore, vary significantly with secretory site location, see figure 10 or equations (3.14 c and d). On the other hand, the distribution

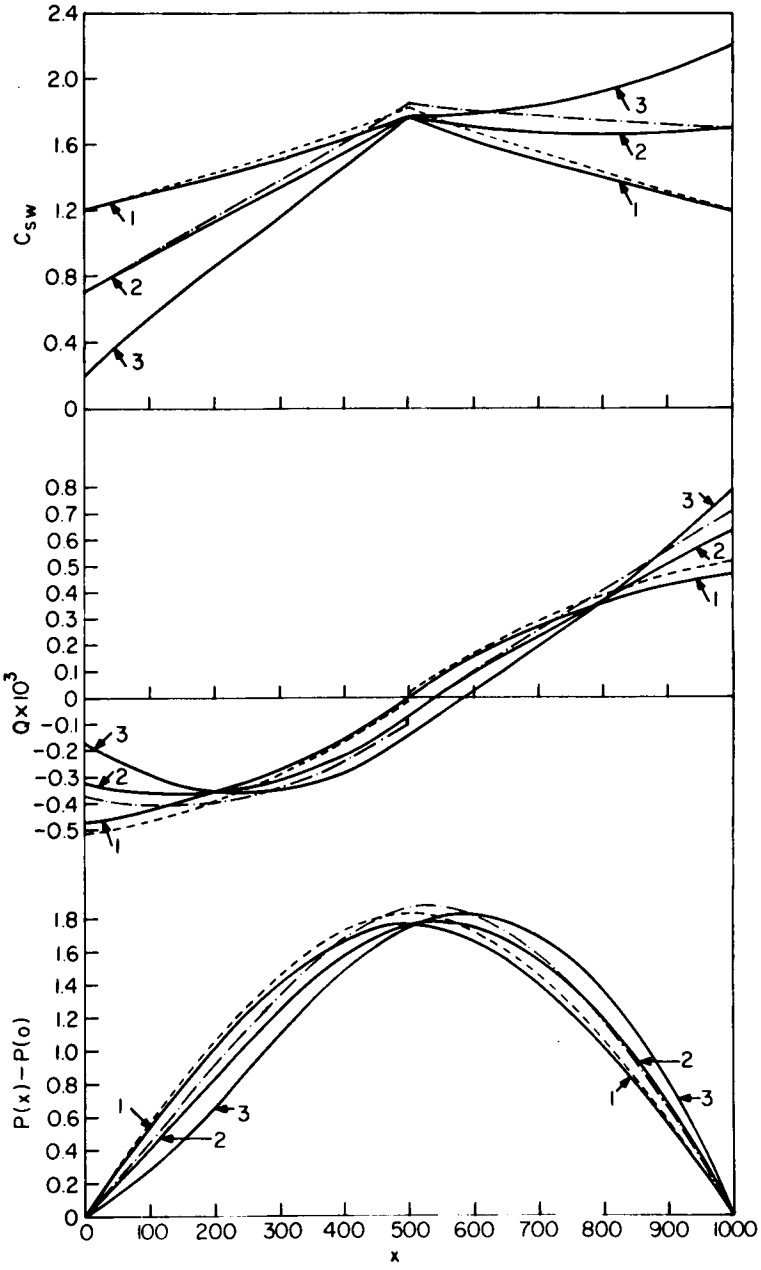

Figure 8. Effect of ΔC_{sw} on the Distributions of Solute Concentration (a), Volume Flux (b) and Pressure (c) in an Open Geometry Channel with Secretory Site Located between $490 < X < 510$. Curve (1): $\Delta C = 0$; Curve (2): $\Delta C = 1.0$; Curve (3): $\Delta C = 2.0$ Comparison with approximate analytical solution for point source secretory site: ----, $\Delta C = 0$; -·-·-·, $\Delta C = 1$. $\epsilon = .872 \times 10^{-2}$, $\eta = 1.345 \times 10^{-6}$, $R = .116 \times 10^{-3}$

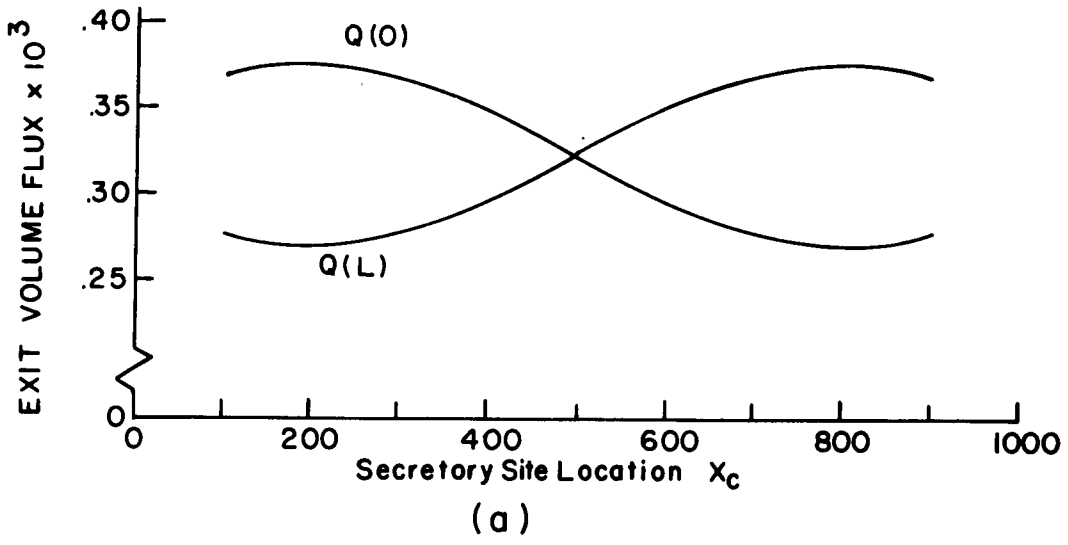

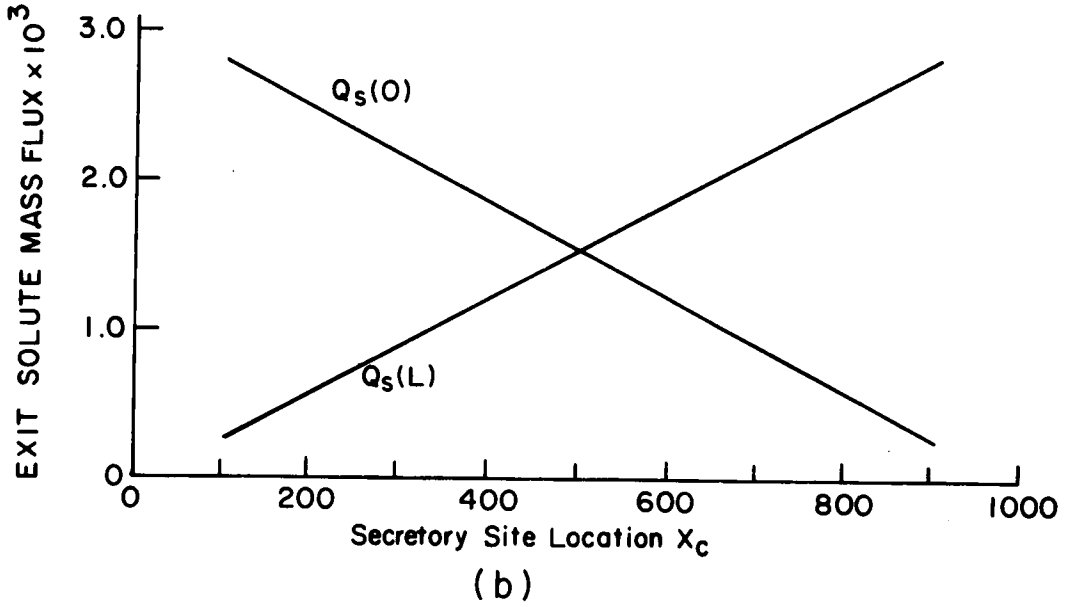

Figure 9. Effect of Location of the Center of the Secretory Site on the Volume Fluxes (a) and Solute Mass Fluxes (b) at the end stations of an Open Geometry Channel with $\Delta P = \Delta C_{sw} = 0$; Secretory Site Length: 100; $\epsilon = .872 \times 10^{-2}$, $\eta = .269 \times 10^{-6}$, $R = .116 \times 10^{-3}$

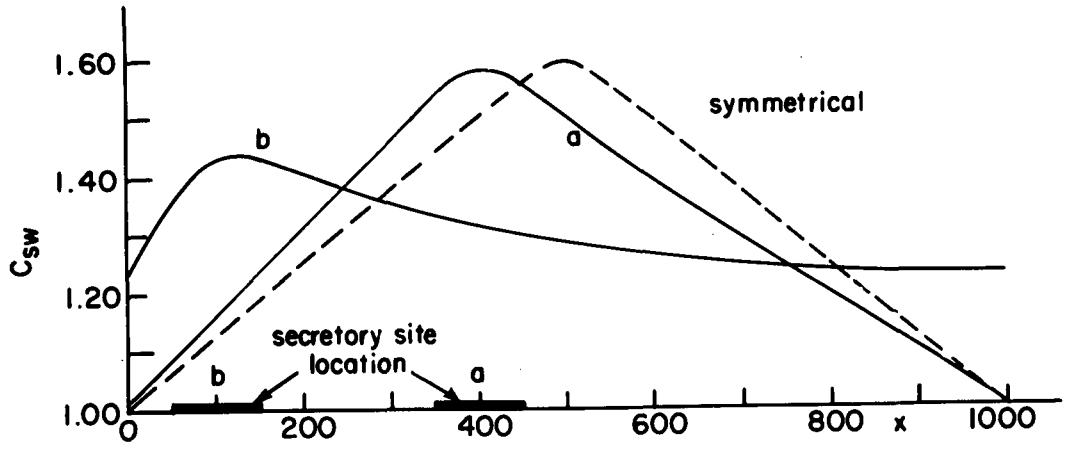

Figure 10. Effect of Secretory Site Location on the Solute Concentration Distribution in an Open Geometry Channel with $\Delta P = \Delta C_{sw} = 0$ and Constant Passive Water Flux; $\epsilon = .872 \times 10^{-2}$, $\eta = .269 \times 10^{-6}$, $R = .116 \times 10^{-3}$

of the water flux out the channel ends is primarily controlled by the filtration pressure differential and not the concentration distribution. One recalls from figure 8c that changes of 0(1) in the concentration profile produced relatively small changes in the pressure distribution provided $\Delta P = 0$.

Figures 6 through 10 are based on hypothetical open channel geometries and boundary conditions in which we have examined separately the effects of the various driving forces and the secretory site location on the water and solute flux distribution within the channel. In figures 11 a and b these various elements have been combined in an attempt to quantitatively model a real membrane, the rabbit ciliary body epithelium. This membrane has been selected since there exists a detailed set of experimental measurements Cole (1961), (1962) which can be used to assess the validity of the theoretical model. These include measurements of the exit volume and solute fluxes and the active transport component of the solute flux for both excised and in vivo rabbit ciliary body epithelia. The theoretically predicted values for these fluxes could be reasonably extrapolated from the results for a single channel using the measured total area of the membrane and an estimate of the average cell and channel dimensions. These dimensions were obtained from observation of high resolution electronmicrographs; these same observations gave an average dimensionless channel length $L = 925$.

For excised preparations Cole found the exit volume and solute fluxes were equivalent, respectively to $Q(L) = .173 \times 10^{-3}$ and $Q_s(L) = .155 \times 10^{-3}$. The latter value was based on the measured short-circuit current, that is the equivalent electron current measured when a low resistance shunt is placed across the membrane and the transmembrane

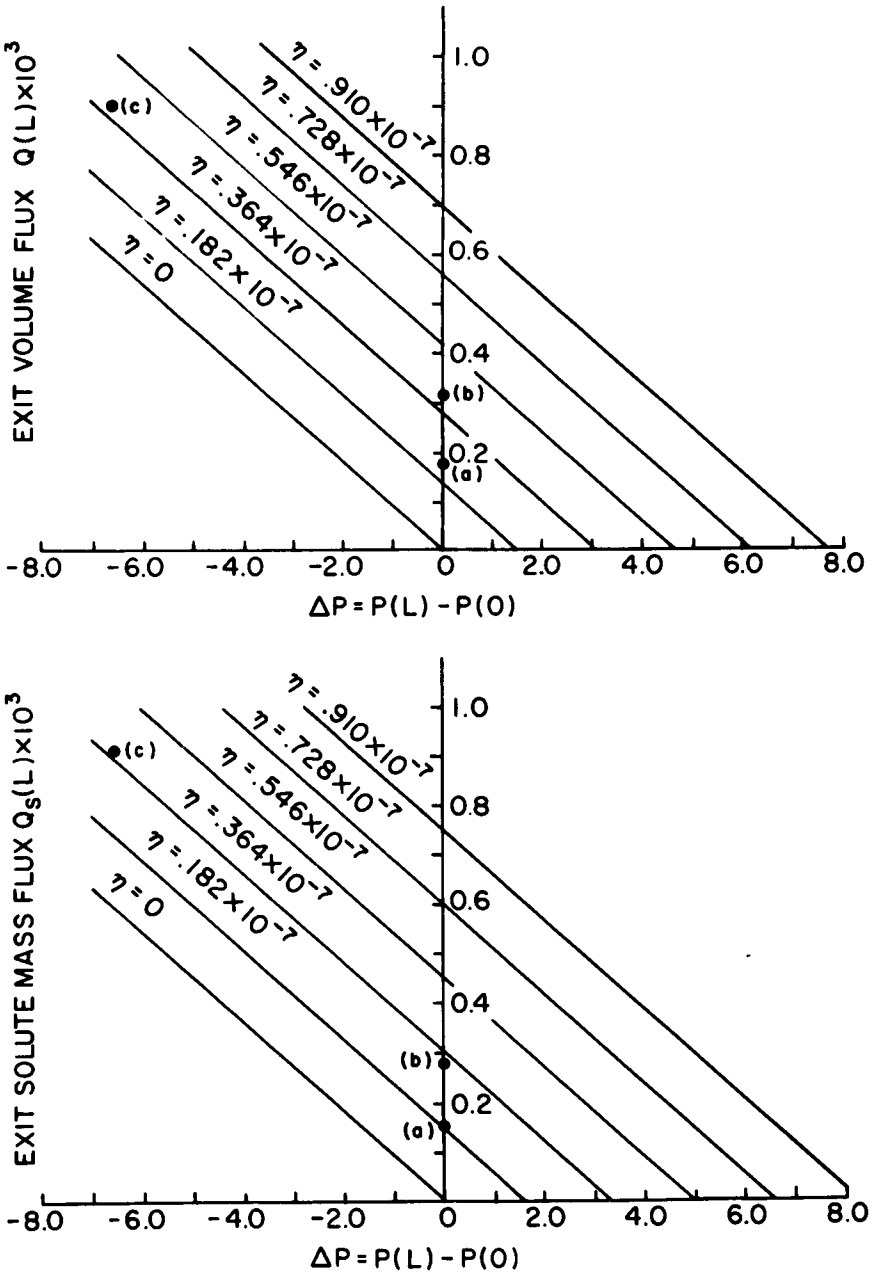

Figure 11. Effect of ΔP and η on the Exit Volume Flux (a) and Exit Solute Mass Flux (b) in an Open Geometry Channel with the Secretory Site Located between $690 < X < 790$; $L = 925$; $\epsilon = .872 \times 10^{-2}$; $R = .0156$ Point (a): Cole's experimental data invitro; Point (b): Estimate of Invivo flux with no filtration; Point (c): Cole's experimental data invivo.

potential difference reduced to zero. These data points are labeled (a) in figures 11 a and b and since $\Delta P = 0$, lie on the vertical axis. The in vivo ΔP is the pressure difference between the intraocular pressure and the blood diastolic pressure in the capillary bed. For the in vivo eye Cole obtained values equivalent to $Q(L) = .9 \times 10^{-3}$, $Q_s(L) = .91 \times 10^{-3}$ and from the short circuit current an active transport component of $Q_s(L) = .28 \times 10^{-3}$. It is to be noted that both the measured volume and solute fluxes in vivo were more than five fold greater than in the excised preparation while the active transport component increased by less than a fector of 2. This intriguing behavior is one of the fundamental unanswered questions in ciliary body transport.

The curves in figures 11 a and b represent the theoretical solutions for the exit volume and solute fluxes in a channel with active transport and pressure filtration but isotonic end stations. The secretory site was centered at x = 740 which places it at the beginning of the apical infoldings of the non-pigmented cell layer, see figure 2; this is the location suggested by histochemical studies of (Na + K) ion dependent ATPase activity. The ion pump strength η is treated as a fixed parameter and is determined by the experimentally measured short circuit current. The appropriate η curve corresponding to Cole's in vitro ($\Delta P = 0$) experiments with the excised eye is shown as point (a) in figure 11b. This value of η is $.182 \times 10^{-7}$. Similarly, ϵ is measured. Only R of the three-dimensionless groups η, ϵ and R is not accurately known. To circumvent this difficulty R was chosen by curve fitting one of the three experimental points in figure 11 a for the volume flux, namely point (c). Thus, two of the six experimental points in figures 11a and b are used to determine the free parameters in the governing equations, while the remaining four points are a true test of the theoretical model. To obtain the theoretically

predicted volume flux the intersection of the $\eta = .182 \times 10^{-7}$ curve with the $\Delta P = 0$ axis is located in figure 11a. The predicated value $Q(L) = .142 \times 10^{-3}$ is within 20 percent of the measured volume flux $Q(L) = .173 \times 10^{-3}$. In view of the uncertainty in the dimensionless group R, the neglect of electrical effects and other model refinements this agreement between theory and experiment is satisfactory.

The in vivo results cannot be compared directly with the in vitro data but must first be corrected for the increased active transport that results from the increased metabolism. It is evident, however, from the curves in figure 11a and b that for the prescribed values of η, ϵ and R the fluxes and driving forces are linearly related. Thus, the active transport component of the total volume flux in the living eye, Q(L) when $\Delta P = 0$, can be determined assuming a linear relation between the in vitro and in vivo short circuit current measurements and the corresponding in vitro volume flux. Q(L) with $\Delta P = 0$ for the in vivo eye is shown as point (b) in figure 11a and has the value $.313 \times 10^{-3}$. The new value of η corresponding to the increased active transport rate is, therefore, about $.4 \times 10^{-7}$. Since η remains constant, the experimentally measured volume flux $Q(L) = .9 \times 10^{-3}$, point (c) in figure 11a is achieved for a dimensionless interstitial-intra-ocular pressure differential $\Delta P = -6.6$, the minus sign appearing because of the direction in which the pressure difference is measured. In dimensional units this ΔP is equivalent to 80 mm of Hg, which when corrected for the small osmolarity differences between blood plasma and aqueous humor gives an equivalent ΔP of approximately 50-60 mm Hg. Returning to figure 11b one notes that the theoretical predictions for the exit solute flux for $\eta = .4 \times 10^{-3}$ are $Q_s(L) = .94 \times 10^{-3}$ for $\Delta P = -6.6$, while $Q_s(L) = .33 \times 10^{-8}$ when $\Delta P = 0$, the

theoretically predicted active transport component. The corresponding experimentally measured values, points (c) and (b) respectively, are $Q(L) = .91 \times 10^{-3}$ and $Q_s(L) = .28 \times 10^{-3}$, the latter being based on the short-circuit current measurement. Both values are obviously in as close an agreement with the theory as one is justified to expect considering the sophistication of the quantitative model.

In, summary the theoretical model predicts that the marked increase in fluid transport in the living rabbit eye compared with that in the dead rabbit eye is due to the hydrostatic pressure difference between the blood and the aqueous humor. These results when combined with the earlier experiments of Davson (1953), which showed that p. amino hippinate M. W 194 and raffinose M. W. 594 could pass with equal facility through the ciliary body epithelium, and Langham's (1958), (1959) intraocular pressure experiments with cat eyes provide cogent evidence that the extracellular channels in the ciliary process are open and provide the transport route for the observed water and solute movement. In contrast to previous qualitative models which attributed the bulk water movement solely to active transport, the present quantitative model shows that the formation of aqueous humor is a pressure dependent mechanism and that the ion pumps are responsible for only about one-third of the total water movement. Results not shown indicate that this active transport fraction is even less for cat eyes, where it accounts for about one-tenth of the total flux.

6. Partial Occulsions

The results of sections 3, 4 and 5 have been confined to constant height extracellular channels. However, as noted in the introduction, electronmicrographs of the ciliary body epithelium clearly indicate localized

regions in which the channel is partially occluded. In this section we shall briefly consider the effect of such constrictions on the streamwise pressure and concentration distribution within the channel. To simplify the analysis we shall assume that there is no active solute transport in the obstructed region and that on the length scale ℓ of the obstruction, the passive movement of water across the lateral boundaries can be neglected. We shall assume, in addition that the inertial forces within the occlusion are small compared to the viscous forces, that the normal component of the momentum equation can be neglected, and that the concentration varies only as a function of x, the instantaneous mixing hypothesis invoked in section 3.

Introducing the simplifications outlined in the last paragraph, impermeable lateral boundaries and a uniform concentration profile, (2.22) and (2.23) become

$$\frac{2}{3}\frac{d}{dx}(U_m h) = 0 \tag{6.1}$$

$$\frac{2}{3}\frac{d}{dx}(U_m h C_s) - \frac{d}{dx}\left(h \frac{dC_s}{dx}\right) = 0 \tag{6.2}$$

Substituting (6.1) into (6.2) and using (2.26a)

$$\frac{d^2 C_s}{dx^2} - \frac{1}{h}\left(Q - \frac{dh}{dx}\right)\frac{dC_s}{dx} = 0 \tag{6.3}$$

One integration of this equation gives

$$\frac{dC_s}{dx} = \frac{C'(0)h(0)}{h} \exp\left(Q \int_0^x \frac{dx}{h}\right) \tag{6.4}$$

where x = 0 here refers to the beginning of the occlusion, $C'(0) = \frac{dC_s(0)}{dx}$

is the initial concentration gradient and Q is a constant in view of (2.26) and (6.1). A second integration yields the final result:

$$C_s(x)-C_s(0) = \frac{C'(0)h(0)}{Q}\{\exp\left(Q\int_o^x \frac{dx}{h}\right) - 1\} \qquad (6.5)$$

The streamwise variation in pressure is obtained from an integration of (2.25), which gives,

$$P(x) - P(0) = -12Q \int_o^x \frac{dx}{h^3} \qquad (6.6)$$

Solutions (6.5) and (6.6) are particularly useful in that they apply to an arbitrary distribution h(x) of channel height. (6.6) is a well known result in lubrication theory.

One convenient form for h(x), which is representative of a typical occlusion geometry is the sinusoidal variation

$$\frac{h(x)}{h(0)} = 1 - \frac{1}{2}\left(1 - \frac{h_t}{h(0)}\right)\left(1 - \cos\frac{2\pi x}{\ell}\right) \qquad (6.7)$$

sketched in the upper left hand corner of figure 11. (6.7) describes a one parameter family of constriction geometries which depend only on the ratio of throat height to initial height $\frac{h_t}{h(0)}$.

Substituting (6.7) into (6.5) and integrating across the constriction one obtains

$$C_s(\ell) - C_s(0) = \frac{C'(0)h(0)}{Q}\left\{\exp\left(\frac{Q\ell}{h(0)}\sqrt{\frac{h(0)}{h_t}}\right) - 1\right\} \qquad (6.8)$$

If (6.8) is now divided by the concentration differential across a uniform section of channel with the same length, initial height and concentration gradient, one has

$$\frac{\Delta C_c}{\Delta C_u} = \frac{\exp\left(\frac{Q\ell}{h(0)}K\right) - 1}{\exp\left(\frac{Q\ell}{h(0)}\right) - 1} \qquad (6.9)$$

where $K = \frac{h(0)}{h_t}$, and ΔC_c ΔC_u represent the concentration differentials for a constricted and unconstricted channel respectively. Similarly, when (6.7) is substituted in (6.6)

$$P(\ell) - P(0) = \Delta P_c = \frac{3}{2} \frac{Q\ell}{h(0)^3} (3K^5 + 2K^3 + 3K)$$

If this result is now divided by the Poiseuille pressure drop ΔP_u across a constant area channel with the same volume flux Q, length ℓ and initial height h(0) one obtains

$$\frac{\Delta P_c}{\Delta P_u} = \frac{3}{8} K^5 + \frac{1}{4} K^3 + \frac{3}{8} K \qquad (6.10)$$

The solution for $\frac{\Delta C_c}{\Delta C_u}$ depends on two dimensionless groups $\frac{Q\ell}{h(0)}$ and K whereas $\frac{\Delta P_c}{\Delta P_u}$ depends only on K. This is not surprising since the convective terms are omitted in the momentum equation (2.25) but are retained in the solute conservation equation (6.2). In the limit as this convective contribution vanishes, $\frac{Q\ell}{h(0)} \to 0$ and $\frac{\Delta C_c}{\Delta C_u}$ in (6.9) becomes only a function of K, as observed in figure 12.

Equations (6.9) and (6.10) have been plotted in figure 12. Since the pressure gradient in a uniform channel is constant the ratio $\frac{\Delta P_c}{\Delta P_u}$ can be interpreted as the ratio of the length of a uniform channel required to produce a pressure drop equal to that across the occluded zone to the length of the occluded zone. The constriction also produces an increased concentration differential; however, this effect is much less pronounced than that for the pressure field for the same value of $\frac{h(0)}{h_t}$, provided $\frac{Q\ell}{h(0)} \leq 0(1)$. For constrictions typical of the ciliary body epithelium, one can anticipate results very close to the limiting behavior for $\frac{Q\ell}{h(0)} = 0$.

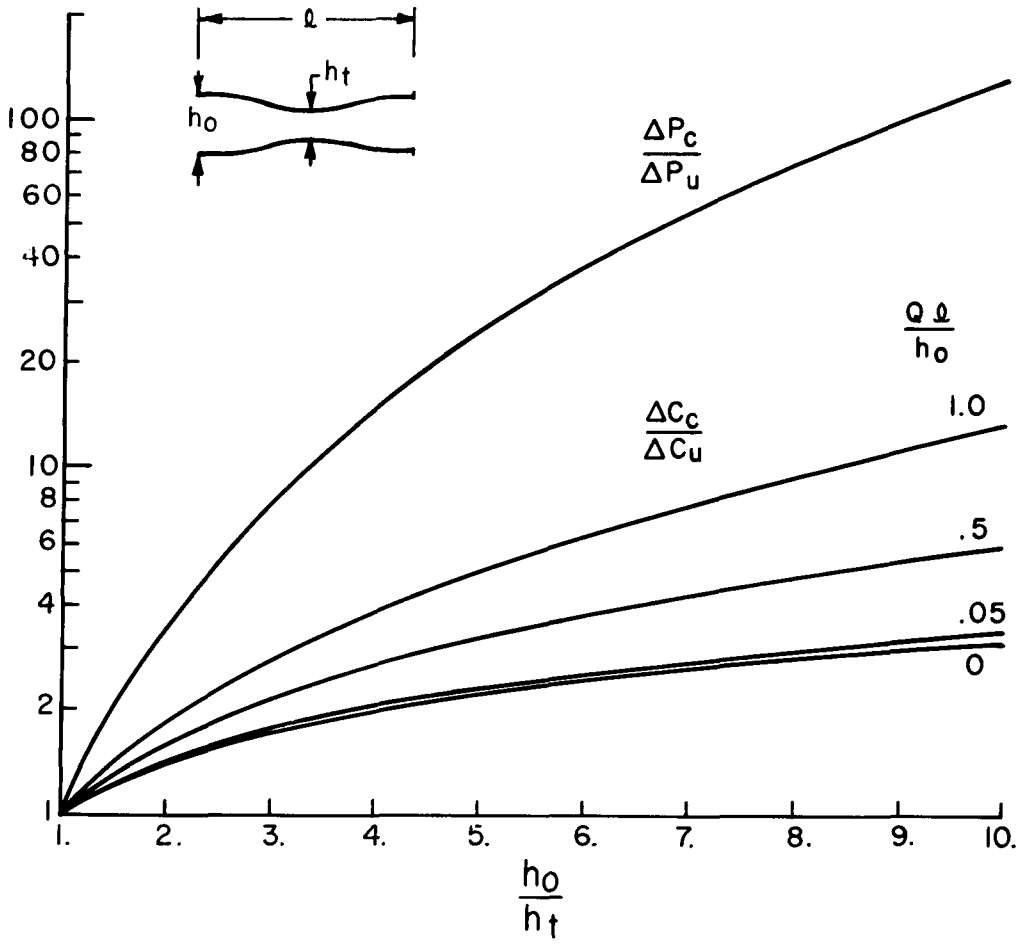

Figure 12. Effect of a Partial Occlusion on the Streamwise Pressure and Concentration Gradient across an Open Geometry Channel.

Equation (6.8) can also be used to show the importance of convection in a constant area channel. To derive this condition we set $\frac{h(0)}{h_t} = 1$ in (6.8) and divide by the linear concentration drop $\Delta C_{Q=0} = C'(0)L$ that would occur in a purely diffusive channel ($Q = 0$) of length L.

$$\frac{\Delta C_u}{\Delta C_{Q=0}} = \frac{h(0)}{QL}\left[\exp\left(\frac{QL}{h(0)}\right) - 1\right] \tag{6.11}$$

For $\frac{QL}{h(0)} << 1$ the ratio in (6.11) is given approximately by

$$\frac{\Delta C_u}{\Delta C_{Q=0}} = 1 + \frac{1}{2}\left(\frac{QL}{h(0)}\right) \tag{6.12}$$

The deviation from the purely diffusive solution predicted by (6.11) or (6.12) is an underestimate since it neglects the passive water movement at the lateral boundaries. These results clearly show that even if $Q << 1$ convective effects will eventually become important if the channel is sufficiently long for $\frac{QL}{h(0)}$ to be $\geq 0(1)$. This, of course, is the motivation behind the use of the coordinate straining technique employed in section 3.

CHAPTER 3. EXIT MIXING

1. Introduction

This chapter is concerned with obtaining solutions for the velocity and solute concentration distribution resulting from the mixing of an inhomogeneous effluent from a single two dimensional channel with a quiescent outer bathing solution. The domain of mixing occupies a half plane (see Figure 3.) that is bounded by a semi-permeable osmotic membrane in the plane of the exit that allows for passive transport of water but not of solute. We seek matched asymptotic solutions which are uniformly valid on the two inner length scales described in Section 2. of Chapter 1. . These length scales h and $\frac{\rho a}{P_w C_o}$ will be referred to as the near and far fields respectively.

2. Far Field Solution

The governing equations for the far field are the Navier Stokes Momentum equation written in terms of the vorticity $\bar{\omega} = \nabla \times \bar{u}$ to eliminate the pressure term, a continuity equation for the incompressible fluid and a solute conservation equation. In vector form these are, respectively

$$\bar{u} \cdot \nabla \bar{\omega} = \nu \nabla^2 \bar{\omega} \tag{2.1}$$

$$\nabla \cdot \bar{u} = 0 \tag{2.2}$$

$$-D\nabla^2 C + \bar{u} \cdot \nabla C = 0 \tag{2.3}$$

where $\bar{u}$ is the bulk fluid velocity and C is the solute concentration.

On the length scale of the far field the Stokes jet emerging from the channel exit appears as a point source of strength a, located at the origin of the polar coordinate system (r,θ) shown in Figure 3. The radial and circumferential velocity components are then both of the order of

magnitude of the convective velocity from the source. From the work of Birkhoff and Zarantonello (1957), the radial velocity in a two dimensional Stokes jet which satisfies a no-slip boundary condition is of the order a/r. Equations (2.1 - 2.3) are therefore non-dimensionalized by defining the dimensionless variables:

$$u^* = \frac{u}{a/r} \; ; \; v^* = \frac{v}{a/r} \; ; \; R = \frac{r}{k} \; ; \; C^* = \frac{C}{C_o} \; ; \; f = \frac{\psi}{a} \tag{2.4}$$

where u and v are the velocity components in the r and θ directions respectively and are related to the two dimensional stream function ψ by

$$u = \frac{1}{r} \frac{\partial \psi}{\partial \theta} \; , \; v = - \frac{\partial \psi}{\partial r} \tag{2.5}$$

k is used to represent the outer length scale $\rho a / P_w C_o$ and f is a dimensionless stream function. All quantities defined in (2.4) are of order unity.

Substitution of (2.4) into (2.5) yields

$$u = \frac{\partial f}{\partial \theta} \; , \quad v = - R \frac{\partial f}{\partial R} \tag{2.6}$$

where asterisks in (2.6) and in all subsequent discussion have been dropped. Equation (2.1) can be written in terms of the dimensionless velocity components as

$$\frac{a}{\nu} \left\{ u \left[R^2 v_{RR} - R v_R + v_{\theta\theta} + 2 u_\theta \right] + v \left[R v_{R\theta} - u_{\theta\theta} \right] \right\} =$$

$$R^3 v_{RRR} - R^2 v_{RR} + R v_R + 2R v_{\theta\theta R} - 4 v_{\theta\theta} - 4 v_\theta - u_{\theta\theta\theta} \tag{2.7}$$

The subscripts in (2.7) indicate partial differentiation in the usual manner.

Since $a/\nu << 1$, and $R = 0(1)$ one obtains after substituting (2.6) into (2.7) the biharmonic equation in polar coordinates,

$$R^4 f_{RRRR} + 2R^3 f_{RRR} - R^2 f_{RR} + R f_R + 2R^2 f_{RR\theta\theta} - 2R f_{R\theta\theta} + f_{\theta\theta\theta\theta} = 0 \quad (2.8)$$

Substitution of (2.5) and (2.6) into (2;3) yields,

$$-R^2 C_{RR} - RC_R - C_{\theta\theta} + \xi R f_\theta C_R - \xi R f_R C_\theta \quad (2.9)$$

where $\xi = a/D$.

We seek solutions of (2.8) and (2.9) subject to the boundary conditions that the solutions are symmetrical about $\theta = 0$, that the no-slip condition is satisfied at the outer membrane $\theta = \pm \frac{\pi}{2}$ and that the mass flux of water crossing this boundary is proportional to the osmotic driving force. This latter condition is written as

$$v\Big|_{\pi/2} = - R(C-1)\Big|_{\pi/2} \quad (2.10)$$

A compatability condition, defining membrane semi-permeability, must also be imposed on the concentration gradient $\frac{\partial C}{\partial \theta}$ and the water flux v at the outer membrane to require that the net solute flux due to convection and diffusion be zero. The diffusional flux of solute $J_{S\theta}$ in the θ direction is assumed to be linearly related to the concentration gradient

$$J_{S\theta} = - M_S D \frac{C_o}{k} \frac{1}{R} \frac{\partial C}{\partial \theta} \quad (2.11)$$

When the sum of (2.11) and the convective solute flux produced by the

velocity v in (2.10) are equated to zero, one obtains

$$\frac{\partial C}{\partial \theta}\Big|_{\theta = \pi/2} = -\xi R C(C-1)\Big|_{\theta = \pi/2} \tag{2.12}$$

The difficulty in solving (2.8) and (2.9) arises primarily through the coupling introduced in the boundary condition (2.10). We therefore formulate the solutions for the stream function and solute concentration as coordinate expansions in R, where the zeroth order solutions are those for which this boundary condition is homogeneous.

We assume that,

$$f = f^{(0)} + R f^{(1)} + 0(R^2) \tag{2.13a}$$

$$C = C^{(0)} + R C^{(1)} + 0(R^2) \tag{2.13b}$$

where $f^{(i)}$ and $C^{(i)}$ are function of θ only.

Substitution of (2.13 a and b) into (2.8) and (2.9) and equating terms of like order in R yields to zeroth order.

$$4 f^{(0)}_{\theta\theta} + f_{\theta\theta\theta\theta} = 0 \tag{2.14a}$$

$$C^{(0)}_{\theta\theta} = 0 \tag{2.14b}$$

To first order in R one has:

$$f^{(1)}_{\theta\theta\theta\theta} + 2 f^{(1)}_{\theta\theta} + f^{(1)} = 0 \tag{2.15a}$$

$$C^{(1)} + C^{(1)}_{\theta\theta} - \xi C^{(1)} f^{(0)}_{\theta} + \xi f^{(1)} C^{(0)}_{\theta} = 0 \tag{2.15b}$$

With a similar substitution into the boundary conditions, (2.10) does not appear to zeroth order and (2.12) produces a homogeneous boundary condition on $C_\theta^{(0)}$.

To first order in R (2.10) and (2.12) become.

$$f^{(1)} \Big|_{\theta = \pi/2} = (C^{(0)} - 1) \Big|_{\theta = \pi/2} \tag{2.16 a}$$

$$C_\theta^{(1)} \Big|_{\theta = \pi/2} = - \xi C^{(0)} (C^{(o)} - 1) \Big|_{\theta = \pi/2} \tag{2.16 b}$$

The solution of (2.14a) satisfying the condition of symmetry at $\theta = 0$ and no-slip at $\theta = \pi/2$ is equivalent to the Stoke's jet solution with radial st eamlines as obtained by Birkhoff and Zarantonello (1957). In the variables defined by (2. 4), this solution becomes

$$f^{(0)} = \frac{\beta_1}{2} (\sin 2\theta + 2\theta) \tag{2.17 a}$$

where β_1 is a constant representing the channel source strength. The solution of (2.14b) satisfying the symmetry condition is

$$C^{(0)} = \beta_2 \tag{2.17 b}$$

where β_2 is a constant to be determined by matching with the near field solution. A first order correction to the streamline pattern is produced by the passive water movement across the outer membrane and is obtained from (2.15a) after applying (2.16 a) and the symmetry and no-slip boundary conditions; One has

$$f^{(1)} = (\beta_2 - 1) \sin \theta \tag{2.18}$$

When the results (2.17 a and b) and (2.18) are substituted into (2.15 b) the governing equation for the first order correction to the uniform concentration field becomes

$$C^{(1)}_{\theta\theta} + [(1 - \xi\beta_1) - \xi\beta_1 \cos 2\theta]\ C^{(1)} = 0 \qquad (2.19)$$

(2.19) is the Mathieu equation and since $\xi << 1$ it can be solved by a small parameter expansion of the form

$$C^{(1)} = C_1 + \xi\beta_1 C_2 + \theta\ (\xi\beta_1)^2 \qquad (2.20)$$

On substituting (2.20) into (2.19) and equating like terms in $\xi\beta_1$

$$C_1'' + C_1 = 0 \qquad (2.21a)$$

$$C_2'' + C_2 = (1 + \cos 2\theta)\, C_1 \qquad (2.21b)$$

When the even solutions to (2.21a and b) are substituted into (2.20) one obtains

$$C^{(1)} = A_1 \cos\theta + \xi\beta_1 [A_2 \cos\theta + \tfrac{3}{4}A_1\,\theta \sin\theta - \tfrac{1}{16}A_1 \cos 3\theta] + 0(\xi\beta_1)^2 \qquad (2.23)$$

where A_1 and A_2 are constants of integration. These are evaluated by taking the derivative of (2.23) with respect to θ, setting the result equal to the right hand side of (2.16 b) and equating terms in like powers of ξ. The first order solution for the concenetration is then found to be

$$C^{(1)} = \xi\beta_2(\beta_2 - 1)\cos\theta \qquad (2.24)$$

Substitution of (2.17 a) and (2.18) into (2.13 a), and of (2.17 b) and (2.24) into (2.13 b) yields finally,

$$f = \frac{\beta_1}{2}(\sin 2\theta + 2\theta) + R\,(\beta_2 - 1)\sin\theta + 0(R^2) \qquad (2.25\,a)$$

$$C = \beta_2 + R\,[\,\xi\,\beta_2(\beta_2(\beta_2-1)\cos\theta + 0(\xi^2)\,] + 0(R^2) \qquad (2.25\ b)$$

One observes in (2.25 a and b) that the passive water movement across the outer membrane produces a first order correction of order R, to the streamline pattern but only a higher order correction, of order ξ R, to the concentration field.

Since the solution (2.25 b) cannot satisfy the initial concentration distribution at the channel exit, we now seek a near field solution which satisfies appropriate initial conditions at the exit and which can be matched term by term with the far field solution in the limit as R approaches zero and the near field radial coordinate approaches infinity.

3. Near Field Solution

The streamline pattern and concentration distribution in the near field obey the governing equations (2.1) through (2.3) subject to boundary conditions which are analogous to (2.10) and (2.12) and to initial conditions at the channel exit. Förste (1963) has obtained closed form analytical solutions to (2.1) and (2.2) for low Reynolds number flow in the half plane $x \geq 0$ (in Figure 3) for arbitrary normal velocity distributions along x= 0. The tangential velocity component is made to satisfy the no-slip condition and therefore vanishes at this boundary. These solutions are not, directly applicable to the current problem because the concentration profile and therefore the normal velocity profile along x= 0 in the region exterior to the channel exit are not known at the outset. One might reasonably, however, neglect the passive water movement across x= 0 in the domain r= 0(h) and use Forste's results for the case in which a jet with a Poiseuille velocity profile emerges from a finite channel into a quiescent outer bathing solution with homogeneous boundary conditions on the velocity at x= 0 and

$\frac{h}{2} \geq y \geq -\frac{h}{2}$. These solutions because of their complexity, would still present severe mathematical difficulties if they were used to define the convective velocity in (2.3).

We proceed, therefore, with the approximate, yet mathematically tractable, approach of using a near field expansion of the far field velocity distribution as the near field convective velocity. This velocity field represents a correct description of the far field and a qualitatively reasonable description as one approaches the exit region. One anticipates thereby, that the resulting solution for the solute concentration field will provide a reasonable representation of the mixing process in the exit region.

We introduce a dimensionless near field radial coordinate

$$r^* = \frac{2r}{h} = \frac{2k}{h} R \tag{3.1}$$

which represents a stretching of the coordinate system in the near field region.

Substitution of (3.1) into (2.25 a and b) then yields

$$f = \frac{\beta_1}{2} (\sin 2\theta + 2\theta) + \frac{hr}{k^2} (\beta_2 - 1) \sin\theta + 0\left[\left(\frac{h}{k}\right)^2\right] \tag{3.2a}$$

$$C = \beta_2 + \frac{h}{k}\frac{r}{2}\left[\xi \beta_2 (\beta_2 - 1) \cos\theta + \theta(\xi^2)\right] + 0\left[\left(\frac{h}{k}\right)^2\right] \tag{3.2b}$$

where the asterisks in r have been dropped.

In order to match (3.2b) with the near field concentration solution, we formulate the latter as a double asymptotic expansion in integral powers of $\frac{h}{k}$ and ξ. We will consider this to be a proper representation of the near field if matching can be accomplished and if boundary conditions can be satisfied to at least the order of approximation associated with

the assumed near field streamline pattern in (3.2 a). We let

$$C = C_0 + \frac{h}{k}\, C_1 + \left(\frac{h}{k}\right)^2 C_2 + 0\left[\left(\frac{h}{k}\right)^3\right]$$

where

$$\begin{aligned} C_0 &= C^{00} + \xi\, C^{01} + 0(\xi^2) \\ C_1 &= C^{10} + \xi\, C^{11} + 0(\xi^2) \\ C_2 &= C_{20} + \xi\, C^{21} + 0(\xi^2) \end{aligned} \tag{3.3}$$

The ordering of terms in (3.3) is, according to the magnitudes given in Section 1

$$1 >> \frac{h}{k} >> \xi >> \left(\frac{h}{k}\right)^2 >> \frac{h}{k}\,\xi \ldots$$

On using (3.1) and the remaining dimensionless variables defined in (2.4), the solute conservation equation (2.3) and the boundary conditions (2.10) and (2.12) for the near field are respectively

$$-r^2 C_{rr} - r C_r - C_{\theta\theta} + \xi\, r f_\theta C_r - \xi f_r C_\theta = 0 \tag{3.4}$$

$$v\Big|_{\theta=\pi/2} = -\frac{h}{k}\,\frac{r}{2}\,(C-1)\Big|_{\theta=\pi/2} \tag{3.5}$$

$$C_\theta\Big|_{\theta=\pi/2} = -\xi\frac{h}{k}\,\frac{r}{2}\,C(C-1)\Big|_{\theta=\pi/2} \tag{3.6}$$

If we define the domain of the near field as that bounded by $\frac{\pi}{2} \geq \theta \geq -\frac{\pi}{2}$ and $r \geq 1$, we can avoid the difficulty associated with solving this boundary value problem with mixed boundary conditions for concentration along the plane $x = 0$. In addition to (3.5) and (3.6) we require that C be bounded for large r, that $C = g(\theta)$, an arbitrary but even function, on $r = 1$, and that the first term in (3.2 a) account for the total volumetric flux emerging from the channel.

In dimensionless form, the latter condition is satisfied by

$$\frac{\beta_1}{2} \int_{-\pi/2}^{\pi/2} \frac{\partial}{\partial\theta} (\sin 2\theta + 2\theta)\, d\theta = 1 \tag{3.7}$$

On integrating (3.7) one finds that

$$\beta_1 = \frac{1}{\pi} \tag{3.8}$$

Substitution of (3.3) into (3.4), (3.5), and (3.6) yields, after equating terms in like powers of $\frac{h}{k}$ and ξ, the equations and boundary conditions to be satisfied by the unknown functions C^{ij} in (3.3).

To order unity:

$$\nabla^2 C^{00} = 0 \tag{3.9 a}$$

$$C^{00}\Big|_{\theta=\pi/2} = 0 \tag{3.9 b}$$

where ∇^2 is the Laplacian in polar coordinates.

We also require that the initial condition on r=1 be satisfied identically to first order. That is

$$C^{00}\Big|_{r=1} = g(\theta) \tag{3.9 c}$$

The even solution to (3.9 a) satisfying (3.9 b), (3.9 c) and the condition of boundedness is

$$C^{00} = A^{00} + \sum_{n=1}^{\infty} F_n^{00} r^{-2n} \cos 2n\theta \tag{3.9 d}$$

where A^{00} and F_n^{00} are the Fourier coefficients

$$A^{00} = \frac{2}{\pi} \int_0^{\pi/2} g(\theta)\, d\theta$$

$$F_n^{00} = \frac{4}{\pi} \int_0^{\pi/2} g(\theta) \cos 2n\theta\, d\theta \quad \text{for } n = 1, 2, 3, \ldots \tag{3.9 e}$$

The solutions of order $\left(\frac{h}{k}\right)^m$ for m=1, 2, ... satisfy Laplace's equation and homogeneous boundary conditions on $\theta = \frac{\pi}{2}$ and r = 1. Therfore

$$C^{10} = C^{20} = C^{m0} = 0 \tag{3.10}$$

According to (3.10), one does not expect to find terms of order R^m appearing in the far field concentration expansion. R will appear only as a mixed product with the parameter ξ.

To order ξ one must solve the equation

$$\nabla^2 C^{01} = r \beta_1 (\cos 2\theta + 1) C_r^{00} \tag{3.11a}$$

subject to homogeneous boundary and initial conditions. Homogeneous solutions of (3.11 a) of the form $r^j \cos j\theta$ are not sufficiently general to satisfy the boundary and initial conditions. We must add to the series in integral powers of r an associated separable solution of order one. This solution is defined as

$$\frac{\partial^n}{\partial j^n} (r^j \cos j\theta) \qquad \text{For } n = 1$$

Separable solutions of any order are seen to satisfy Laplace's equation since

$$\nabla^2 \frac{\partial^n}{\partial j^n} (r^j \cos j\theta) = \frac{\partial^n}{\partial j^n} \nabla^2 (r^j \cos j\theta) = 0$$

The complete solution to (3.11a) using the result of (3.8) is given by

$$C^{01} = A_1^{01} + \sum_{n=1}^{\infty} A_n^{01} r^{-2n} \cos 2n\theta + \sum_{n=1}^{\infty} \frac{F_n^{00}}{2\pi} r^{-2n} \left[\frac{n}{2(2n+1)} \cos(2n+2)\theta \right.$$

$$\left. - \frac{n}{2(2n-1)} \cos(2n-2)\theta + \ln r \cos 2n\theta \right] \tag{3.11b}$$

where $A_1^{01} = \frac{F_1^{00}}{4\pi}$

$$A_n^{01} = \frac{1}{4\pi}\left[\frac{(n+1)F_{n+1}^{00}}{(2n+1)} - \frac{(n-1)F_{n-1}^{00}}{(2n-1)}\right] \qquad \text{for } n = 2, 3, 4, \ldots$$

If (3.9 d), (3.10) and (3.11 b) are substituted into (3.3) and the resulting series is rewritten in terms of the outer coordinate R by use of (3.1), a comparison of the three leading terms (of order unity, $\frac{h}{k}$, and ξ) with the corresponding terms in (2.25b) yields the matching condition

$$\beta_2 = A^{00} + \frac{\xi F_1^{00}}{4\pi} \tag{3.12}$$

The results (3.10) and (3.12) show that the functions $C^{(i)}$ in (2.13 b) are in fact power series expansions in the parameter ξ.

There is no justification for obtaining solutions of order $\frac{h}{k}\ \xi$ because the assumed stream function (3.2 a) does not satisfy boundary condition (3.5) to this order. The final approximate solution has, therfore, not included the higher order corrections due to the passive water movement across the outer boundary.

4. Numerical Results

The far field streamline patterns resulting from different levels of exit concentration are most conveniently represented as lines of constant stream function in a polar coordinate system whose radial dimension is the quantity $R(\beta_2 - 1)$ or $R(1-\beta_2)$ for hypertonic (i.e. $\beta_2 > 1$) or hypotonic ($\beta_2 < 1$) channel secretions respectively. Equations (2.25 a), using (3.8), is plotted in this manner in Figures 13 and 14 One observes that the radial streamline pattern ensues as R approaches zero or as the channel secretion approaches isotonicity ($\beta_2 = 1$). In these limits the streamlines for $f = \pm 0.5$ become tangent to the boundary $\theta = \pm \frac{\pi}{2}$.

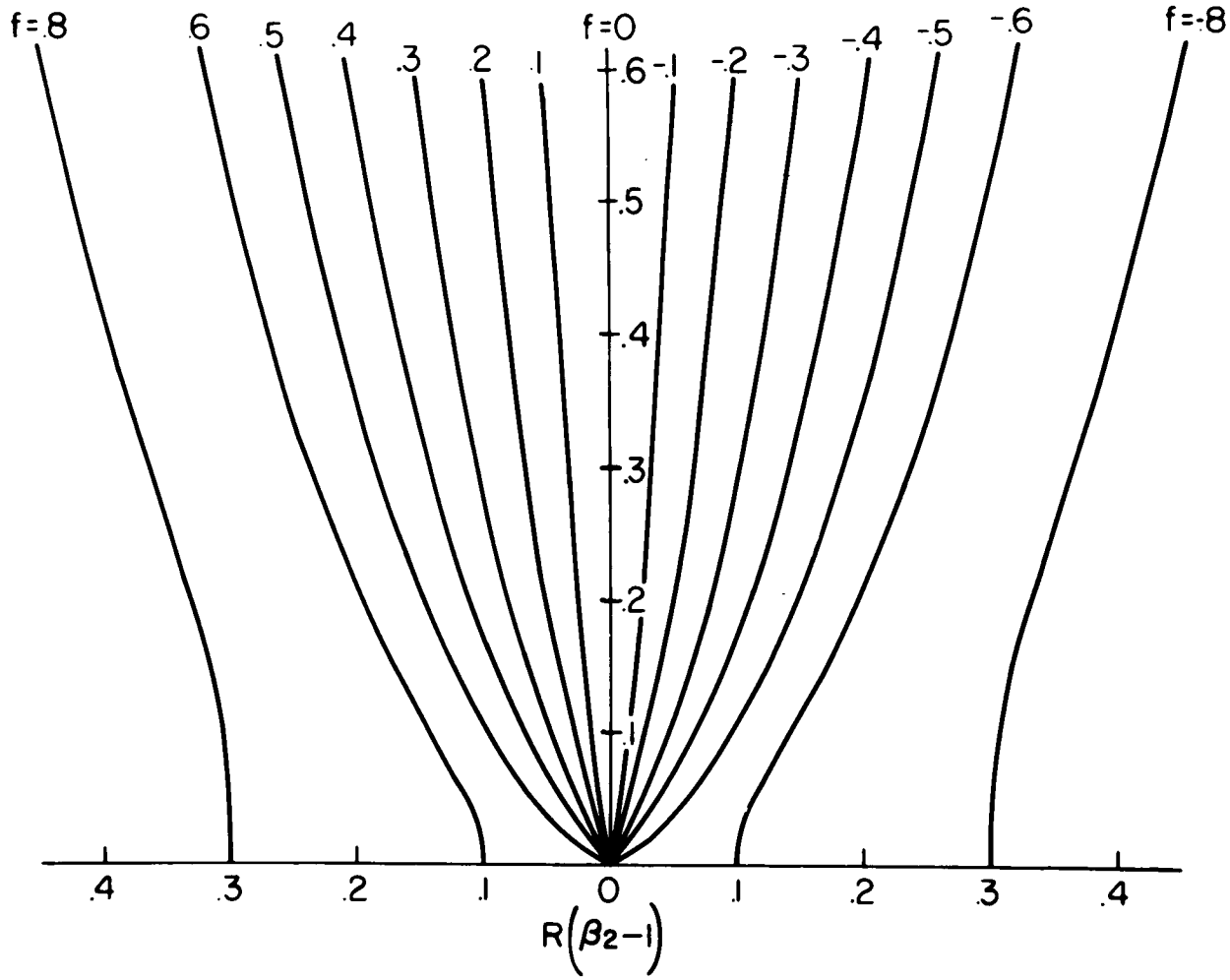

Figure 13. Streamline Pattern in Exit Mixing Region of Epithelia with Hypertonic Effluent.

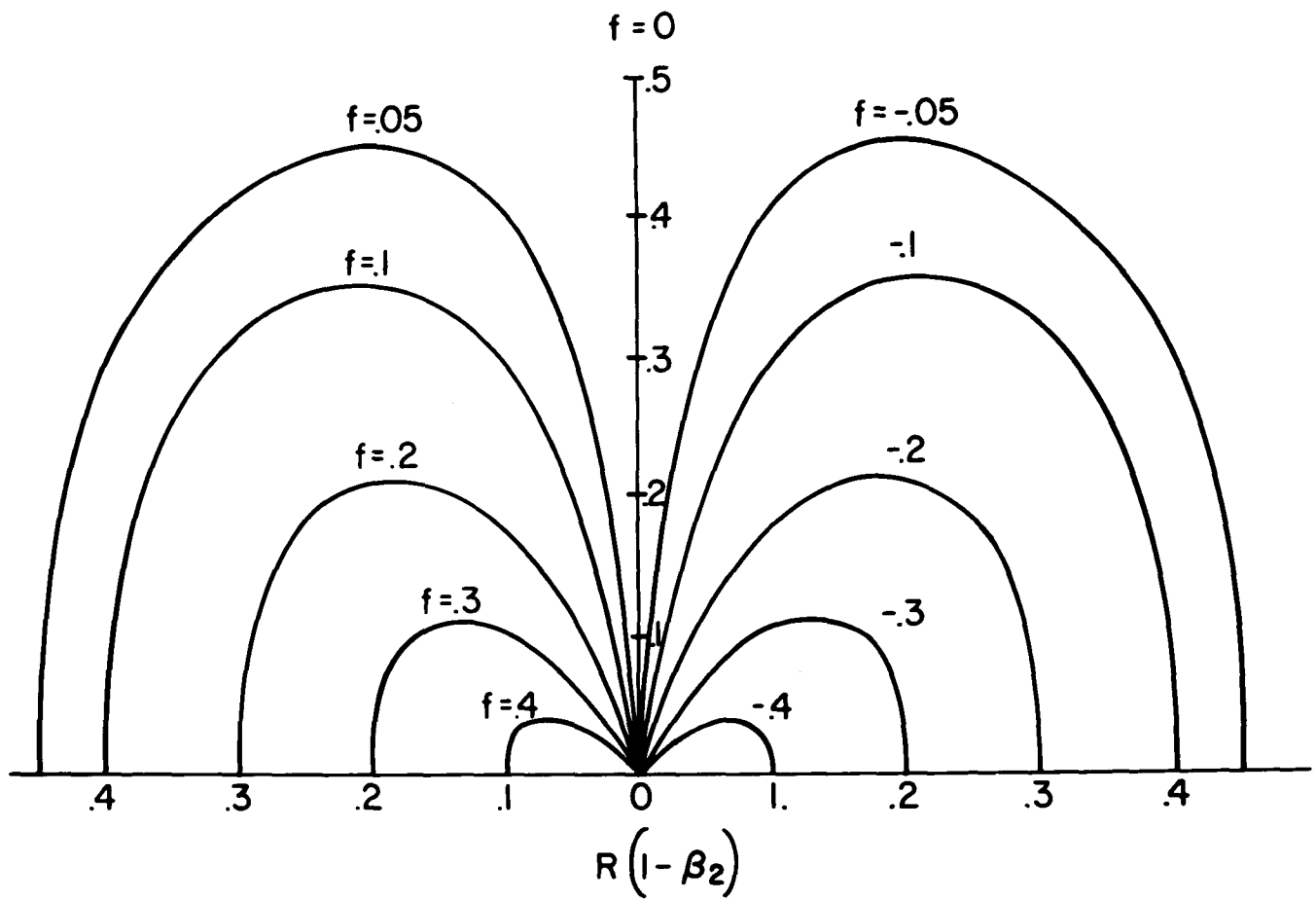

Figure 14. Streamline Pattern in Exit Mixing Region of Epithelia with Hypotonic Effluent.

The radial length scale in Figure 13 and 14 also represents, to first order, the ratio of the volumetric flow crossing the outer boundary to the channel source strength. In dimensionless terms one has that

$$\frac{Q_e}{a} = \int_0^R \frac{\partial f}{\partial R}\, dR \quad \text{on } \theta = \frac{\pi}{2} \tag{4.1}$$

Substitution of (2.25 a) and (3.8) into (4.1) yields on integration

$$\frac{Q_e}{a} = R\,(\beta_2 - 1) + \ldots \tag{4.2}$$

Where the positive direction of Q_e is taken as the positive x direction in Figure 3.

Equation (2.25 b) may be represented by lines of constant concentration ratio $\frac{C}{\beta_2}$ in a polar coordinate system with radial length scale $R\,\xi\,|(\beta_2 - 1)|$. Then from (2.25 a)

$$\frac{C}{\beta_2} = 1 + R\,\xi\,(\beta_2 - 1)\cos\theta + \ldots \tag{4.4}$$

Lines of constant concentration in (4.4) lie parallel with the outer membrane, which has a concentration ratio of 1. With β_2 greater or less than unity, the concentration increases or decreases, respectively with increasing x, with a uniform gradient of + or -1.

5. Conclusions

The development of theories for biological jets presents the fluid dynamicist with new and relevant areas for research. Several classes of problems can be identified according to the relative magnitudes of the dimensionless groups which characterize the flow. Most epithelia appear to transport fluids at rates which make the dimensionless groups a/ν and a/D much less than unity. Biological jets are, then, low Reynolds number jets in which the length scales of interest are h, $\rho a/P_w C_o$, λ, and a radius

of curvature $\mathcal{R}$ of the epithelial surface.

For a relatively impermeable outer cell membrane, $\rho a/P_w C_o$ becomes much larger than the channel spacing λ and additional transport across this membrane can be neglected. The problem then involves the study of an array of jets emerging into the outer bathing solution. Work on a solution for this model has been started by the author. New mathematical techniques are needed for the case in which $\rho a/P_w C_o$ is of the order of the channel height. The work of Forstë (1963) may however, provide a basis for solution.

Since the epithelial tissue forms a closed surface which lines the various organs, the choice of a coordinate system most compatable with the physiological configuration is is related to the magnitude of the dimensionless parameter $\mathcal{R}/L$, where L is one of the characteristic length scales described above. For $\mathcal{R}/L \gg 1$ the model is best formulated as a half plane in either rectangular or polar coordinates. For the gall bladder, as presented herein, $\mathcal{R}/L \gg 1$ for each of the three characteristic length scales. In mammelian renal collecting tubules, see Grantham (1971), $\mathcal{R}/L = 0(1)$ when L represents the extracellular channel spacing. In this case a formulation in axisymmetric coordinates is called for.

The transport processes occurring in renal tubules and in the malpighian tubules and rectal lumen of insect excretory systems, see Wall (1971), Oschman and Berridge (1971), present problems with non-stagnant bathing solutions. In organs such as these, the epithelia line the lumenal surface of long cylindrical tubes which are closed at one end. The absorption or secretion of fluids then occurs across epithelia which are bounded on one side by the serosal fluid and on the lumenal side by a bathing solution which has unidirectional flow velocities. The coordinate system chosen to represent this model again depends on $\mathcal{R}/L$.

APPENDIX

APPENDIX

We present here the second order corrections of order $(\epsilon R)^2$, to the approximate analytical solution for the pressure and volume flux distributions derived in Section 3 of Chapter 2. The boundary conditions for the second order set of equations (3.13) are homogenous for $P_{1,2}^{(2)}$ and $Q_{1,2}^{(2)}$. With the matching conditions derived from (3.5 a and c) one obtains:

$$Q_1^{(2)} = \{ -\frac{2}{5}\alpha_1^2 X_o^5 - \alpha_1(\frac{5}{2}C(0)-2)X_o^4 - \frac{2}{3}[(C(0)-1)(5C(0)-2)+\alpha_1\alpha_3]X_o^3$$
$$+[\alpha_5-\alpha_3C(0) - (C(0)-1)(\frac{2C(0)(C(0)-1)}{\alpha_1}+\alpha_3)]X_o^2$$
$$+\frac{2C(0)-1)}{\alpha_1}[\alpha_5-\alpha_3C(0)]X_o\} + \alpha_9 \quad \text{for } 0 < X_o < L_{os} \qquad \text{(i)}$$

$$Q_1^{(2)} = \{ -\frac{2}{5}\alpha_2^2 X_o^5 - \alpha_2(\frac{5}{2}C(0)+\frac{5}{2}SL_{os}-2)X_o^4 - \frac{2}{3}[(C(0)+SL_{os}-1)(5C(0)+5SL_{os}-2)$$
$$+\alpha_2\alpha_4]X_o^3 + [\alpha_5-\alpha_4(C(0)+SL_{os}) - (C(0)+SL_{os}-1)(\frac{2(C(0)+SL_{os})(C(0)+SL_{os}-1)}{\alpha_2}$$
$$+\alpha_4)]X_o^2 + 2\frac{(C(0)+SL_{os}-1)}{\alpha_2}[\alpha_5-\alpha_4(C(0)+SL_{os})]X_o\} + \alpha_{10}$$
$$\text{for } L_{os} < X_o < L_o \qquad \text{(ii)}$$

$$P_1^{(2)} = 12\{\frac{7}{30}\alpha_1^2 X_o^6 + \frac{\alpha_1}{10}[14C(0)-11]X_o^5 + [\frac{2}{3}\alpha_1\alpha_3 + (C(0)-1)(\frac{17}{6}C(0)-\frac{4}{3})]X_o^4$$
$$+[\frac{\alpha_3}{3}(8(C(0)-5) + \frac{2C(0)}{\alpha_1}(C(0)-1)^2 - \frac{2}{3}\alpha_5]X_o^3 + \frac{2(C(0)-1)}{\alpha_1}(\frac{3}{2}\alpha_3C(0)-\alpha_5)$$
$$+\frac{\alpha_3^2}{2}]X_o^2 + [\frac{\alpha_3^2C(0)}{\alpha_1} - \frac{\alpha_3\alpha_5}{\alpha}]X_o\} - 12\alpha_9 X_o$$

$$\text{for } 0 < X_o < L_{os} \qquad \text{(iii)}$$

$$P_1^{(2)} = 12\Big\{\frac{7}{30}\alpha_2^2 X_o^6 + \frac{\alpha_2}{10}[14C(0)+14SL_{os}-11]X_o^5 + [\frac{2}{3}\alpha_2\alpha_4$$

$$+ (C(0)+SL_{os}-1)(\frac{17}{6}(C(0)+\frac{17}{6}SL_{os}-\frac{4}{3})]X_o^4 + [\frac{\alpha_4}{3}(8C(0)+8SL_{os}-5$$

$$+ \frac{2(C(0)+SL_{os})}{\alpha_2}(C(0)+SL_{os}-1)^2 - \frac{2}{3}\alpha_5]X_o^3 +$$

$$[\frac{2(C(0)+SL_{os}-1)}{\alpha_2}(\frac{3}{2}\alpha_4 C(0)+\frac{3}{2}\alpha_4 SL_{os}-\alpha_5)+\frac{\alpha_4^2}{2}]X_o^2+[\frac{\alpha_4^2}{2}(C(0)+SL_{os})$$

$$-\frac{\alpha_4\alpha_5}{\alpha_2}]X_o\Big\} - 12\alpha_{10}X_o + \alpha_{11}$$

for L_{os} X_o L_o (iv)

where

$$\alpha_9 = \frac{1}{L_o}[\{iv\}_{X_o=L_o} + \{iii\}_{X_o=L_{os}} - \{iv\}_{X_o=L_{os}}$$

$$\alpha_{10}=\alpha_9 + \{i\}_{X_o=L_{os}} - \{ii\}_{X_o=L_{os}}$$

$$\alpha_{11}= 12\left[\{iii\}_{X_o=L_{os}} - \{iv\}_{X_o=L_{os}}\right] + 12L_{os}\left[\{i\}_{X_o=L_{os}} - \{ii\}_{X_o=L_{os}}\right]$$

The symbols {i}, {ii}, {iii}, {iv} refer to the terms contained within the curely brackets in equations (i), (ii), (iii), and (iv) respectively.

LIST OF REFERENCES

REFERENCES

Birkhoff, G.; Zarantonello, E.M. (1957) Jets Wakes and Cavities, Academic Press, 272

Bittar, E.E. (1970) Membranes and Ion Transport, Wiley Interscience

Cole, D.F. (1961), Brit. J. Ophthalmal. 45, 202.

Cole, D.F. (1962), Brit. J. Ophthalmal. 46, 577

Davson, H. (1953), J. Physiol. 122, 10P.

Diamond, J.M. (1964), J. Gen. Physiol. 48, 15.

Diamond, J.M. and Bossert, W.H. (1967), J. Gen. Physiol. 50, 2061

Diamond, J.M. and Tormey, J.M. (1966), Nature 210, 817.

Forste, J. (1963) Zeitschrift fur Angewandte Mathematik und Mechanic 43, 353

Grantham, J.J. (1971) Federation Proceedings, 30, No. 1, 14

Langham, M.E. (1958), Physiol. Rev. 38, 215.

Langham, M.E. (1959), J. Physiol. 147, 29.

Oschman, J.L., Berridge M.J. (1971) Federation Proceedings, 30 No 1, 49

Segel, L.A. (1970), J. Ther. Biol. 29, 233.

Stein, W.D. (1967) The Movement of Molecules Across Cell Membranes, Academic Press

Wall, B.J. (1971) Federation Proceedings 30, 42

AUTOBIOGRAPHICAL STATEMENT

J.Richard Goldgraben was born on March 15, 1934 in New York City. He attended the public schools in the New York suburb of Long Beach and entered the Cornell University Sibley School of Mechanical Engineering in September 1951. Upon graduating with a degree of Bachelor of Mechanical Engineering in June 1956 he volunteered for the U.S. Navy and attended the Naval Officer Candidate School in Newport Rhode Island. He subsequently served as a Ship Superintendent and Assistant Planning Officer at the Naval Shipyard, Long Beach, California. On release from active duty he returned to Cornell University and was awarded the degree of Master of Mechanical Engineering in June 1960. From June 1960 to June 1965 he served as a Principal Engineer in the Department of Mechanical Engineering of the Columbus, Ohio laboratories of the Battelle Memorial Institute. He joined the faculty of the Mechanical Engineering Department of the Polytechnic Institute of Brooklyn in September 1965, a position which he holds at the time of this writing. He began his doctoral studies in Fluid Dynamics at the City College of the City University of New York in September 1967 and was a recipient of a National Science Foundation Science Faculty Fellowship in 1970.